ANNUAL REVIEWS

Annual Review of Physiology

Endoplasmic Reticulum–Plasma Membrane Junctions as Sites of Depolarization-Induced Ca^{2+} Signaling in Excitable Cells

Rose E. Dixon and James S. Trimmer

Department of Physiology and Membrane Biology, School of Medicine, University of California, Davis, California, USA; email: jtrimmer@ucdavis.edu

Annu. Rev. Physiol. 2023. 85:217–43

First published as a Review in Advance on October 6, 2022

The *Annual Review of Physiology* is online at physiol.annualreviews.org

https://doi.org/10.1146/annurev-physiol-032122-104610

Keywords

membrane contact sites, second messenger, ion channel, skeletal muscle, cardiac muscle, smooth muscle, neuron

Abstract

Membrane contact sites between endoplasmic reticulum (ER) and plasma membrane (PM), or ER-PM junctions, are found in all eukaryotic cells. In excitable cells they play unique roles in organizing diverse forms of Ca^{2+} signaling as triggered by membrane depolarization. ER-PM junctions underlie crucial physiological processes such as excitation-contraction coupling, smooth muscle contraction and relaxation, and various forms of activity-dependent signaling and plasticity in neurons. In many cases the structure and molecular composition of ER-PM junctions in excitable cells comprise important regulatory feedback loops linking depolarization-induced Ca^{2+} signaling at these sites to the regulation of membrane potential. Here, we describe recent findings on physiological roles and molecular composition of native ER-PM junctions in excitable cells. We focus on recent studies that provide new insights into canonical forms of depolarization-induced Ca^{2+} signaling occurring at junctional triads and dyads of striated muscle, as well as the diversity of ER-PM junctions in these cells and in smooth muscle and neurons.

INTRODUCTION

Specialized membrane contact sites (MCS) between endoplasmic reticulum (ER) and the inner face of the plasma membrane (PM), termed ER-PM junctions, allow for events occurring within the limiting membrane of the cell to impact ER function and vice versa (1–3). In excitable cells this includes coupling the effects of rapid changes in membrane potential that occur with electrical activity to ER function, which can reciprocally impact PM function, including membrane excitability. ER-PM junctions play crucial roles in diverse aspects of physiology across all eukaryotic cell types, including prominent roles in lipid signaling and homeostasis and as sites for diverse forms of Ca^{2+} signaling (1–6). While many of these functions of ER-PM junctions are conserved in all eukaryotic cells, including excitable cells, there exist specialized structures, molecular compositions, and functions of ER-PM junctions unique to excitable cells. In particular, ER-PM junctions in excitable cells are specialized to mediate unique modes of Ca^{2+} signaling triggered by membrane depolarization.

Numerous molecules have been identified that contribute to the generation and maintenance of ER-PM junctions in mammalian cells (1, 2, 5). One class comprises resident ER integral membrane-tethering proteins that bind to specific forms of phosphorylated lipids in the inner leaflet of the PM, including junctophilins (JPHs), extended synaptotagmins, and vesicle-associated membrane protein-associated proteins (VAPs). The other class is pairs of integral PM and ER proteins whose interacting cytoplasmic domains form the contacts between the two membranes. To date the known pairings involve a PM polytopic ion channel (an Orai Ca^{2+} channel or a K_V2 K^+ channel) interacting with a single transmembrane segment resident ER protein (a stromal interaction molecule or STIM protein, or VAP, respectively). ER-PM junctions of both classes form functional microdomains that mediate distinct forms of Ca^{2+} signaling (3).

Here, we review recent research findings on the structure, molecular composition, and function of ER-PM junctions in forming specialized microdomains for Ca^{2+} signaling in excitable cells, with a primary focus on striated and smooth muscle and neurons. We discuss similarities and differences between these structures and functions in different excitable cell types. Although important roles of ER-PM junctions in mediating events triggering excitation-contraction (E-C) coupling in skeletal muscle and cardiomyocytes were established many decades ago, more recent studies have revealed the richness of proteins that establish and regulate the structures that underlie these events. Moreover, studies in other excitable cells have revealed similarities but also important cell type–specific distinctions in the structure and function of ER-PM junctions.

ENDOPLASMIC RETICULUM–PLASMA MEMBRANE JUNCTIONS IN MUSCLE CELLS

Though they likely exist in all eukaryotic cells, ER-PM junctions were originally discovered in electron microscope (EM) images in a 1957 study examining the ultrastructure of skeletal and cardiac muscle cells (7). The terms dyads (two-element) and triads (three-element) were applied to describe the arrangement of junctional sarcoplasmic reticulum (jSR) alongside periodic, sarcomere-adjacent, invaginating tubules of PM known as transverse tubules (t-tubules). As they engage SR, the specialized ER of muscle cells, we refer to dyads and triads as SR-PM junctions. Triads are the predominant SR-PM junctions in skeletal muscle cells, where t-tubules often appear sandwiched between two jSR cisternae (**Figure 1*a***). Dyads are more frequently observed in cardiac muscle cells (**Figure 1*b***). SR-PM junctions are not limited to those involving t-tubules but are also found along axial tubules and at surface sarcolemma in peripheral couplings that predominate in smooth muscle cells (SMCs) (**Figure 1*c***). Interestingly, the number of junctions, their length, and intermembrane distance appear to confer specialization across muscle types according to the

speed, force, and manner of contraction (i.e., phasic or tonic), such that fast-twitch skeletal muscle has the largest number of tightly associated triadic junctions; slow-twitch skeletal and cardiac muscle have fewer, predominantly dyadic junctions, whereas slower, weaker smooth muscle has the fewest and loosest junctions. Here, we discuss how muscle SR-PM junctions are specialized for the primary functional output of contraction and relaxation. We highlight current knowledge on their molecular composition, synthesis, and breakdown.

SKELETAL MUSCLE SARCOPLASMIC RETICULUM–PLASMA MEMBRANE JUNCTIONS

Skeletal muscle SR-PM triads are the primary location of E-C coupling (8), whereby an electrical signal (i.e., an action potential) is transduced into mechanical contraction. Efficient skeletal muscle E-C coupling is required for a plethora of critical, sometimes life-sustaining functions including breathing, movement, chewing, and swallowing. Triads house the ion channel machinery of E-C coupling. This includes PM-localized L-type Ca^{2+} channels (LTCCs), also known as

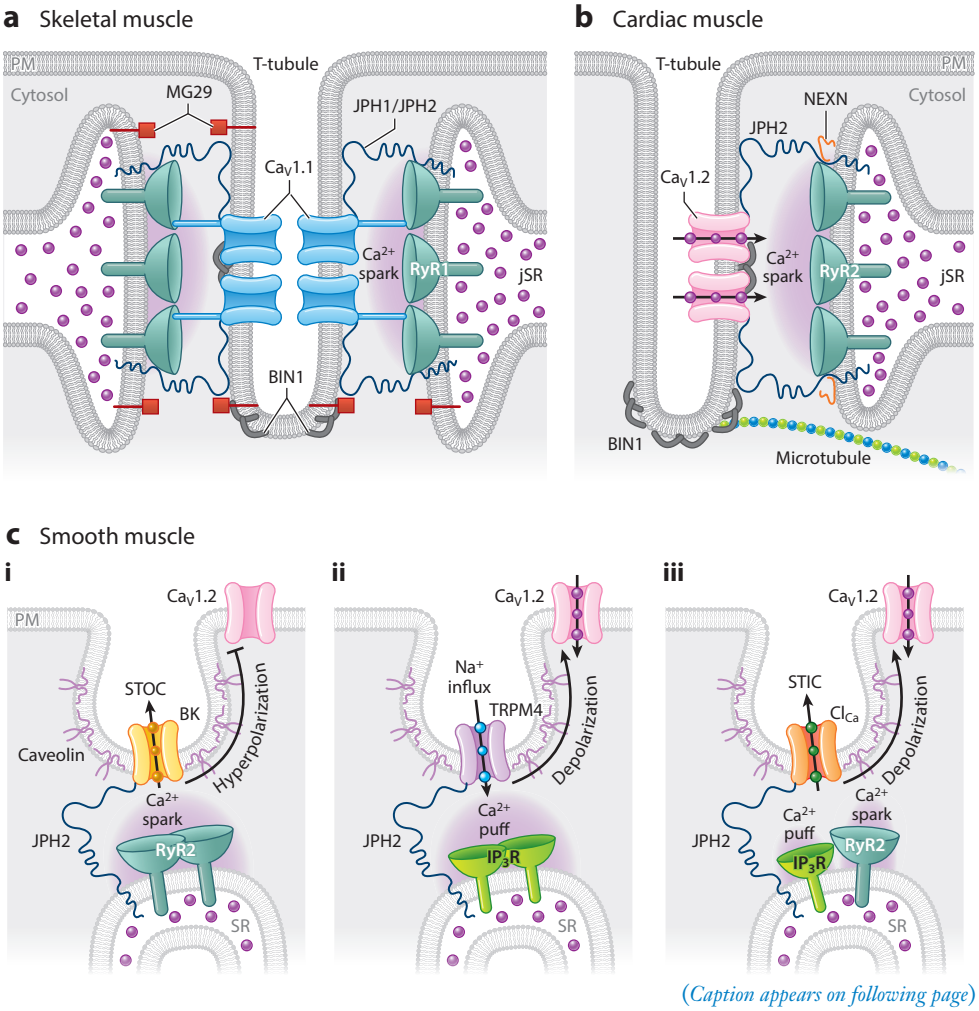

(*Caption appears on following page*)

Figure 1 (*Figure appears on preceding page*)

SR-PM junctions as platforms for depolarization-induced Ca^{2+} signaling in muscle. (*a*) Depiction of a skeletal muscle triad with the typical SR-t-tubule-SR arrangement, where t-tubule-localized $Ca_V1.1$ channels (*blue*) physically interact with jSR-localized RyR1 (*teal*) to orchestrate Ca^{2+} signaling that leads to contraction during action potential–induced depolarizations. Triadic proteins JPH1 and JPH2 (*dark blue*) tether the junctions, while triad morphology is supported by MG29 (*red*) and BIN1 (*gray*). (*b*) A cardiac muscle dyad shows $Ca_V1.2$ channels (*pink*) within nanometer proximity of an SR-localized RyR2 (*teal*). This arrangement facilitates CICR and myocardial contraction. Dyadic proteins NEXN (*orange*), BIN1 (*gray*), and JPH2 (*dark blue*) play roles in dyad regulation, membrane folding, and tethering, respectively. (*c*) Diagram of smooth muscle peripheral couplings, focusing on those between the caveolar PM and peripheral SR. (*c*, *i*) An MCS containing PM BK channels (*yellow*) and ER RyR2 (*teal*) allows for BK channel activation by RyR2-mediated Ca^{2+} release, leading to STOC-mediated membrane hyperpolarization and reduced $Ca_V1.2$ (*pink*) activity favoring smooth muscle relaxation. (*c*, *ii*) An MCS at which activation of PM TRPM4 channels (*purple*) by Ca^{2+} release from closely associated SR IP_3Rs (*green*) triggers Na^+ influx and membrane depolarization that enhance $Ca_V1.2$ (*pink*) activity favoring smooth muscle contraction. (*c*, *iii*) An MCS containing PM Ca^{2+} activated Cl^- channels (*orange*) that are activated by Ca^{2+} release from nearby SR IP_3R (*green*) or RyR (*teal*) triggers STIC that leads to membrane depolarization that activates $Ca_V1.2$ (*pink*) L-type Ca^{2+} channels, leading to smooth muscle contraction. Abbreviations: BIN1, bridging integrator 1 protein; $Ca_V1.1$, L-type Ca^{2+} channel; CICR, Ca^{2+}-induced Ca^{2+} release; ER, endoplasmic reticulum; IP_3R, inositol 1,4,5-trisphosphate receptor; JPH, junctophilin; jSR, junctional sarcoplasmic reticulum; MCS, membrane contact site; MG29, mitsugumin29; NEXN, nexilin; RyR, ryanodine receptor; SR, sarcoplasmic reticulum; SR-PM, sarcoplasmic reticulum–plasma membrane; STIC, spontaneous transient inward current mediated by Ca^{2+}-activated Cl^- channel; STOC, spontaneous transient outward current mediated by Ca^{2+}-activated K^+ channel; TRPM4, transient receptor potential melastatin 4.

dihydropyridine receptors or DHPRs, comprising pore-forming and voltage-sensing $Ca_V1.1$ LTCC α_{1S} subunits complexed with auxiliary subunits (9). On the other side of the triad, juxtaposed SR-localized ryanodine receptors (RyRs; specifically RyR1) constitute the SR-Ca^{2+} release channel portion of the machinery. DHPRs and RyRs physically interact in a complex that bridges the junctional cleft (**Figure 1*a***). Action potentials triggered by excitatory neurotransmission at the neuromuscular junction propagate throughout the muscle fiber sarcolemma and into t-tubules. These brief depolarizing impulses last 2–5 ms and trigger outward movement of the voltage sensor domain of the t-tubule $Ca_V1.1$ channels. Their direct physical interaction allows the conformational change in the DHPRs to be allosterically coupled to activation of RyRs, triggering Ca^{2+} release from the SR via a mechanical mechanism that does not require Ca^{2+} influx through DHPRs (10–13). The elevation in intracellular Ca^{2+} activates myofilaments and generates muscle contraction. Thus, skeletal muscle SR-PM junctions are the structural platforms for transmission of excitation from PM to SR. Signaling at triads is bidirectional, as physical interaction between RyRs and DHPRs also enhances $Ca_V1.1$ activity (12, 14) and slow voltage-gated Ca^{2+} current (I_{Ca}) activation kinetics (14, 15). That a mechanical linkage mediates retrograde RyR1-to-DHPR signaling was demonstrated by its restoration by expression of only the N-terminal cytosolic portion of RyR1 ($RyR1_{1:4300}$) that lacks the ion channel–forming segments in RyR1-null dyspedic myotubes (14).

Given that both orthograde (outside-in, DHPR-to-RyR1) and retrograde (inside-out, RyR1-to-DHPR) signaling pathways require physical association between DHPRs and RyRs, a logical hypothesis was that this interaction tethered the jSR and PM together and was the basis of triad formation. However, triadic junctions are still present in $Ca_V1.1$-null dysgenic mice (16) and RyR1-null dyspedic mice (17). Dyspedic skeletal muscle triads have a smaller gap (~7 nm) between the jSR and t-tubule PM than wild-type (WT) mice (~12 nm) (17). RyRs are the largest known ion channel with a bulky N-terminal cytosolic cap domain that protrudes 10–12 nm from the SR membrane (18, 19), traversing and likely defining the ~12-nm junctional gap at triads (17). RyRs also influence the distribution of DHPRs, which localize to the t-tubule PM opposite

checkboard-like arrays of RyR1, with every other RyR1 associated with a tetrad of DHPRs (20). Although present in bony fish and all higher-order vertebrates (21), such arrays are absent in dyspedic mice where DHPRs are more randomly distributed (17). In summary, the E-C coupling function of the SR-PM junctions in skeletal muscle requires the presence and physical interaction of DHPRs and RyR1. However, these MCS remain in mice lacking expression of one or the other interacting partner, albeit with an altered structure in the absence of RyR1. While triads form and can be captured with EM in dysgenic and dyspedic myocytes, there is little information on their stability or lifetime. Future studies should examine whether a lack of DHPR or RyR1 impacts triad stability.

Skeletal muscle is highly specialized for rapid contraction and relaxation, having a vast SR with a huge Ca^{2+} storage capacity and little intrinsic leak. A high concentration of SR-localized sarco/endoplasmic reticulum Ca^{2+} transporting -ATPase type 1 (SERCA1) exists at triads, meaning Ca^{2+} release is well matched by a rapid reuptake, especially during single-twitch contractions. However, there is still a need for Ca^{2+} entry to ensure Ca^{2+} homeostasis and store repletion during repetitive contractions to avoid muscle fatigue. A specialized form of store-operated Ca^{2+} entry (SOCE), mediated by a complex of ER STIM1 and PM Orai1 proteins, contributes to meeting this need in skeletal muscle, as reviewed recently (22). Although fundamental to the homeostasis of depolarization-induced Ca^{2+} signaling at SR-PM junctions in skeletal muscle, due to space constraints we refer the reader to this review and others on STIM and Orai store-operated Ca^{2+} channels (23, 24), including skeletal myopathies resulting from STIM and Orai mutations (25).

TRIAD FORMATION AND MAINTENANCE

The Role of Mitsugumin29

As previously stated, in skeletal muscle DHPRs and RyRs are not required for the formation of SR-PM junctions. In a calculated effort to identify triad-forming proteins, monoclonal antibodies (mAbs) were developed from mice immunized with rabbit skeletal muscle membrane vesicles (26). One (mAb1007) yielded a striated pattern of immunolabeling in skeletal muscle reminiscent of that of DHPRs and RyR1, with subsequent immunogold electron microscopy confirming that mAb1007 immunolabeling was at triads. The mAb1007 target protein was immunopurified, partially sequenced, subsequently cloned from rabbit skeletal muscle, and named mitsugumin29 (MG29) after a 29-kDa protein of triads (mitsugumi means a triad junction in Japanese). MG29 has four transmembrane segments and is related to the synaptophysin family of proteins that share common functional and structural properties with connexins (27) and that regulate the fusion pore complex where synaptic vesicles form junctional complexes with PM to orchestrate exocytosis (28). This suggested that MG29 could tether SR to PM in skeletal muscle cells, potentially forming a gap-junction-like pore there. Additionally, MG29 expression in amphibian embryos was found to precede t-tubule and triad formation, beginning in SR membranes, and ultimately localizing to triads as they form (29). However, MG29 knockout (KO) mice were found to maintain tethered triads and were viable, surviving into adulthood despite mild reductions in contractile strength and ultrastructural abnormalities in triad junctions including dilated, fragmented terminal SR cisternae and swollen, irregularly aligned t-tubules (30). Therefore, while MG29 appears to play a role in shaping jSR and t-tubule morphology, it is not the critical SR-PM tether.

The Role of Junctophilins

JPHs are ER proteins that act as PM tethers by binding PM phospholipids via membrane occupation and recognition nexus or MORN domains (31). The discovery of JPHs came from a second mAb (mAb2510) isolated from the same screen that identified MG29 (31). mAb2510 also yielded

immunolabeling of triads, and immunopurification of its target protein led to the cloning of JPH1 and its identification as the essential tether of skeletal muscle SR-PM junctions (31). There are four known isoforms of JPH, of which JPH1 [661 amino acids (aa)] and JPH2 (696 aa) are expressed in skeletal muscle (31). These conserved proteins (32) that span the cleft of ER-PM junctions have an N-terminal PM anchor of eight MORN motifs proposed to bind to PM phospholipids, specifically $PI(4,5)P_2$ and phosphatidylserine, and a C-terminal ER transmembrane segment (31, 33, 34). A recent structural study revealed positively charged patches within MORN motifs that could potentially interact with negatively charged phospholipids. However, cocrystallization in high concentrations of $PI(4,5)P_2$ or phosphatidylserine revealed a very low binding affinity for lipids in this in vitro setting (35). The structure also cast doubt on an alternative hypothesis that JPH2 was PM associated due to its palmitoylation (36), as proposed cysteine sites of palmitoylation were either buried and inaccessible or obscured by binding to other proteins (35). JPH1 truncation mutants lacking the C-terminal SR anchor remain PM localized (31), but the exact mechanism of JPH-PM association remains to be fully elucidated. ER-PM junctions that form in response to exogenous expression of JPH1 in amphibian embryos have a mean cleft distance of ~7.6 nm (31), virtually identical to that observed in RyR1-null dyspedic mouse myotubes (17), and they lacked feet structures that would indicate the presence of RyRs. This supports that the large cytosolic cap of RyRs influences the junctional gap distance and hints that elasticity or flexibility in JPH1 allows it to extend to ~12 nm to accommodate RyR1 but still maintain its tethering function.

The importance of JPH1 for triad formation and E-C coupling was demonstrated in JPH1 KO mice that have significantly fewer triadic junctions in skeletal muscle in tongue, jaws, thigh, and diaphragm, and presumably more broadly (37). These mice die within one day of birth (i.e., on postnatal day 1 or P1) as the result of breathing and regurgitation issues due to issues with suckling and feeding that are not rescued by feeding via gastric tubes. In addition, force generation in JPH1-null pup hindlimb muscle was found to be reduced compared to that in WT pups, confirming the importance of JPH1-mediated triad tethering for efficient skeletal muscle E-C coupling and survival. Interestingly, almost all skeletal muscles examined in JPH1 KO mice had an unaltered number of dyadic junctions (37), supporting a role for JPH2 in dyads and JPH1 in triads. Skeletal muscle triads only begin to develop at embryonic day 17 (E17), coincident with upregulation of JPH1 expression (37, 38). In contrast, dyads in skeletal muscle appear at E14 when JPH2 expression is already high (38). The profound issues with suckling and breathing that led to death at P1 suggest a disproportionate vulnerability of jaw muscle and diaphragm to JPH1 KO. Further insights came from studies of triads and dyads in WT and JPH1 KO pups from E17 through P1, extending to P3 for WT pups (38). A steep increase in triad numbers after birth was seen in WT digastric and diaphragm muscles, more so than in hindlimb muscles, reflecting the importance of these muscles in early life-sustaining functions and the deficits in suckling and breathing in P1 JPH1 KO mice. Acute adenovirus-mediated double knockdown of JPH1 and JPH2 with a small hairpin RNA was used to interrogate their role in adult skeletal muscle SR-PM junctions, where triads are in the majority (39). Simultaneous knockdown to 40–60% of normal expression levels of both JPH isoforms led to abnormal alignment of triads and occasionally to the absence of triadic junctions. Taken together, these results strongly support a role for JPH1 and JPH2 in SR-PM tethering in skeletal muscle, with a prominent role for JPH1 in triad development and maintenance.

Physical interactions between $Ca_V1.1$ and RyR1 are essential for skeletal muscle E-C coupling, but how are these proteins concentrated at triads? A new hypothesis for this was raised in recent work (40) where channel accumulation at striated muscle SR-PM junctions was postulated to

occur due to a left behind phenomenon attributed to a lack of access of the endocytic machinery to the confined junctional space. Further studies will be required to test this interesting postulate, but it is notable that elements of the cortical actin scaffold, a key player in endocytosis, are excluded from some ER-PM junctions in neurons (41, 42), where MCS are said to form at holes in the scaffold. Although imaging cortical actin in muscle cells presents more of a challenge owing to the abundance of actin in the sarcomeres, it would be interesting to determine whether a similar exclusion of cortical actin occurs in striated muscle SR-PM junctions and to investigate whether this abrogates endocytosis in triads and dyads. Not mutually exclusive with this hypothesis, a role for JPHs in recruiting and retaining these Ca^{2+} channels to their respective membranes in skeletal muscle triads has been supported by several studies. Co-immunoprecipitation and pulldown experiments performed on rabbit skeletal muscle cell microsomes have revealed a quadripartite complex consisting of $Ca_V1.1$, RyR1, JPH1, and a cholesterol-binding scaffolding protein called caveolin 3 (Cav-3) (43). In the same study, JPH2 was seen to copurify with $Ca_V1.1$. The $Ca_V1.1$ interaction sites were mapped to similar regions on JPH1 (aa 232–369) and JPH2 (aa 216–399), encompassing MORN motifs 7 and 8 and an adjacent region (43), and to the JPH1 interacting region on $Ca_V1.1$ to the proximal C-terminal region of aa 1,595–1,606 (44). Isothermal titration calorimetry experiments recently confirmed the 1:1 stoichiometry between a 16-aa rabbit $Ca_V1.1$ peptide (aa 1,594–1,609) and the first three MORN motifs of JPH1 and JPH2 (35). That these sites on JPH1 and JPH2 are distinct from those originally identified (43) may suggest that the reduced environment of the in vitro experiments influenced the precise nature of protein–protein interactions. The crystal structure of JPH2 in complex with the aa 1,594–1,609 $Ca_V1.1$ peptide revealed several critical interaction interfaces (35). Alanine substitution of three key residues [arginine (Arg)1599, Arg1600, and phenylalanine (Phe)1605] within this region yielded a $Ca_V1.1$ mutant that failed to bind JPH2 and that exhibited reduced clustering (~60%) compared to WT $Ca_V1.1$ when expressed in dysgenic myotubes (35). Small interfering RNA (siRNA) used to knockdown both JPH1 and JPH2 yielded a more profound effect on $Ca_V1.1$ clustering in myotubes (44), suggesting that additional interaction sites may exist outside of these three residues. The double knockdown of JPH1 and JPH2 also significantly reduced RyR1 clustering at SR-PM junctions (44), consistent with the impact of JPH proteins on $Ca_V1.1$ clustering and in agreement with the initial report of JPH1-RyR1 interactions (45). Together, these studies support that JPH1 and JPH2 interactions with $Ca_V1.1$ and RyR1 promote the recruitment and retention of these channels at triads and dyads of skeletal muscle myotubes, but some molecular details remain unelucidated.

If JPH interactions with $Ca_V1.1$ and RyR1 are essential for their localization at skeletal muscle dyads and triads, a logical prediction is that JPH knockdown should be detrimental to E-C coupling. Indeed, double knockdown of JPH1 and JPH2 in myotubes leads to reduced I_{Ca} and diminished amplitude of evoked Ca^{2+} transients (44). Once situated and clustered at stable dyad/triad junctions, the interaction between $Ca_V1.1$ and RyR1 is also facilitated by interaction of the Src homology three and cysteine rich domain type 3 (STAC3) protein with the II–III loop of $Ca_V1.1$ (for a recent review, see 46) and by $Ca_V\beta_{1a}$ (47). Accordingly, conformational coupling of $Ca_V1.1$ and RyR1 has recently been recapitulated in nonmuscle tsA201 (i.e., HEK293T) cells transiently transfected with RyR1, $Ca_V1.1$, STAC3, $Ca_V\beta_{1a}$, and JPH2 (48). Together, these studies show that great progress has been made in defining the components of the specialized SR-PM junctions (triads, dyads) that mediate depolarization-induced Ca^{2+} signaling in skeletal muscle, although further definition of details of the molecular mechanisms and how they are disrupted in disease remain unclear.

CARDIAC MUSCLE SARCOPLASMIC RETICULUM–PLASMA MEMBRANE JUNCTIONS

Junctional dyads constitute the specialized nanodomain for cardiac E-C coupling. In cardiomyocytes, SR-PM junctions form not just at z-lines adjacent to transverse t-tubule membranes but also at peripheral membranes and along axially orientated sarcolemmal tubules. Depending on the age (49) and size of the animal (50, 51), there may be more or fewer dyadic (transverse or axial tubule–associated) or peripheral (surface sarcolemma–associated) populations. In myocytes without an extensive t-tubule network (e.g., atrial myocytes in certain species), peripheral couplings are the site of E-C coupling. At dyadic junctions, clusters of $Ca_V1.2$ LTCCs are concentrated on t-tubules (52–56) within nanometer proximity of their functional RyR2 partners clustered on jSR (**Figure 1*b***). In contrast to skeletal muscle, cardiac myocytes do not have cross-junctional physical linkages between the PM LTCCs and SR RyRs, but their proximity at dyads is still required to ensure their efficient and rapid chemical communication. Action potential depolarization of cardiomyocytes stimulates $Ca_V1.2$ channel opening, leading to a small influx of Ca^{2+} that then triggers Ca^{2+}-induced Ca^{2+} release (CICR) of a larger amount of Ca^{2+}, observed experimentally as Ca^{2+} sparks (57) from the closely apposed RyR2 clusters. Near simultaneous triggering of 20,000–50,000 Ca^{2+} release units across a single myocyte leads to a global elevation in Ca^{2+} sufficient to trigger contraction. Subsequent relaxation is achieved when SERCA2-mediated SR Ca^{2+} uptake and to a lesser extent PM Na^+/Ca^{2+} exchanger–mediated extrusion return intracellular Ca^{2+} concentrations or $[Ca^{2+}]$ to resting levels.

There exists a 12–15-nm dyadic cleft between jSR and PM at these junctions, with an average length of 100–200 nm, and diffusion of cytosolic molecules is restricted within this confined and crowded space (58, 59). As in skeletal muscle, the cytosolic portion of RyR2 protrudes ~12 nm into the cleft, and anywhere from 9 to >100 RyR2s are present per Ca^{2+} release unit (60). $Ca_V1.2$ channels are thought to protrude ~2 nm into the cleft (61), with 1 to >13 $Ca_V1.2$ channels per dyad (56, 62) at an estimated RyR2:$Ca_V1.2$ ratio of 7.3 (63). Along with these SR and PM Ca^{2+} channels, Cav-3, β-adrenergic receptors, associated signaling complexes, and anchoring proteins are also densely packed into dyads. The high density of proteins in such a small space has been suggested to help funnel Ca^{2+} entering through $Ca_V1.2$ channels toward closely apposed RyR2, facilitating high E-C coupling gain and rapid, high-fidelity contraction (58). However, even with multiple $Ca_V1.2$ channels in each dyad, not all of them will open with every depolarization, as $Ca_V1.2$ channels have a maximum open probability of <0.5 (64). However, they manage to consistently trigger CICR from cross-dyad RyR2 during every heartbeat (62). One hypothesis proposed to reconcile this apparent discrepancy involves $Ca_V1.2$ clustering and cooperative gating (55, 65). Concerted opening of multiple $Ca_V1.2$ channels within a cluster, driven by the constituent channel with the highest open probability, amplifies Ca^{2+} influx through PM channels during cardiac action potentials when extremely depolarized (0 to +50 mV) membrane potentials lead to only tiny femtoamp unitary Ca^{2+} currents, which in independently gating channels would be unable to reliably trigger RyR2 openings. Combined with restricted ionic diffusion within dyads, cooperative gating constitutes a fail-safe system for the beating of the heart (66).

Unlike skeletal muscle, contractile force of the heart cannot be graded by activating more neuromuscular junctions. Every single cardiomyocyte participates in every beat of the heart due to the functional syncytium created by their tight electrical coupling. Thus, in the heart, force is graded by the degree of Ca^{2+} release and regulatory pathways that enhance Ca^{2+} influx and/or enhance the Ca^{2+} sensitivity of the RyR2 to generate positive inotropic responses. Recent work has revealed the existence of an endosomal reservoir of $Ca_V1.2$ channels that is rapidly mobilized to enable channel exocytosis into t-tubule membranes during β-adrenergic stimulation (53, 54).

Newly inserted channels form large clusters in which the channels gate cooperatively to amplify Ca^{2+} influx, stimulating larger CICR and eliciting stronger contractions. This provides a mechanism to tune E-C coupling and graded force generation by rapidly increasing expression of $Ca_V1.2$ channels in t-tubule membranes.

DYAD FORMATION AND MAINTENANCE

In mice and rats, t-tubules are not present at birth in ventricular myocytes but begin forming at ~P10, with dyads appearing by P20 (67). In humans t-tubules develop in utero, with dyads evident by 32 weeks of gestation (68). Dyad density and t-tubule network complexity increase with heart rate, reflecting the functional importance of these signaling platforms for rapid, coordinated rises in intracellular Ca^{2+} and accompanying contraction. Accordingly, small mammals such as mice and rats have a higher density of dyads than larger mammals with lower heart rates such as cows, sheep, and humans (69). Accumulating evidence shows that cardiac dyads are highly dynamic structures that undergo constant remodeling and alterations as jSR retracts and emerges in the vicinity of t-tubules (70, 71). Similarly, on the PM side of the dyad, t-tubules exhibit plasticity, particularly during development and disease (69). Although we do not have the complete molecular picture of exactly how t-tubules and dyads are formed, several proteins have been identified as key players including Cav-3, JPH2, amphiphysin II/bridging integrator 1 protein (BIN1), and nexilin (NEXN) (**Figure 1*b***). Cav-3 is concentrated in t-tubules during development (67, 72) and remains a dyad-localized protein as junctions mature into adulthood. However, E-C coupling and Ca^{2+} signaling persist in the face of Cav-3 KO (73), implying that it does not play an essential role in dyad formation or maintenance. Accordingly, here, we focus on the roles of JPH2, BIN1, and NEXN.

The Role of Junctophilin 2

Although both JPH1 and JPH2 are expressed in skeletal muscle, cardiomyocytes express only JPH2 (37), which is the SR protein that tethers cardiac dyads together (74). Transmission EM studies of purified JPH2 revealed an ~15-nm long structure, the approximate width of the dyadic cleft (33). Underscoring its critical role in cardiac development and function, knocking out JPH2 in mice is embryonic lethal between E9.5 and E11.5 when cardiac contractile activity commences (31), coincident with onset of t-tubule formation (67). Furthermore, cardiac-specific silencing of JPH2 in adult mice precipitates heart failure within a week and is associated with more variation in dyadic spacing and an aberrant increase in RyR2 activity (75). Conversely, overexpression of JPH2 has been reported to reduce RyR2 activity (76). These findings point toward a role of JPH2 in stabilizing the closed state of RyR2, which is important in minimizing the occurrence of potentially arrhythmogenic diastolic CICR and SR leak. JPH2 KO mice also have reduced colocalization between $Ca_V1.2$ and RyR2 in ventricular myocytes (75). Ultrastructural analyses revealed that the number of dyads in JPH2 silenced myocytes is 40% lower than controls, whereas JPH2 overexpression produces enlarged RyR2 clusters and dyads (76). These results suggest that JPH2 plays a critical role in dyad maintenance and spacing in adult ventricular myocytes (75). JPH2 also physically interacts with $Ca_V1.2$ and is postulated to play a role in the recruitment and retention of $Ca_V1.2$ channels at dyads (77, 78).

Developmental upregulation of JPH2 expression coincides with t-tubule development and maturation (67), while JPH2 knockdown during development results in disorganized and disrupted t-tubule networks (79). Cardiac-specific JPH2 KO mice fail to form mature t-tubules, whereas overexpression of JPH2 promotes accelerated t-tubule development (80, 81). That failure

to produce t-tubules in developing myocytes occurred despite unaltered BIN1 levels (80) speaks to the profound importance of JPH2 in t-tubule biogenesis and maturation. Many heart failure models exhibit disrupted t-tubule networks that have been linked with JPH2 downregulation in a reversion toward an immature phenotype (79, 82–84). A similar association has been reported in patients with hypertrophic (82), dilated, or ischemic cardiomyopathy (83, 84). *JPH2* mutations are associated with hypertrophic cardiomyopathy in humans (82, 85). Indeed, JPH2 gene therapy has been proposed as a putative heart failure therapeutic, as AAV9-mediated restoration of JPH2 levels in a pressure-overload model of heart failure was found to prevent t-tubule loss and rescue SR Ca^{2+} handling and systolic function (86). However, findings of reduced expression or function of JPH2 are not a generalized feature of heart failure, and some animal models and human heart failure patients show t-tubule network disruption despite normal JPH2 levels (87, 88). These findings suggest that JPH2 is a driver of t-tubule loss in heart failure, but perhaps not the only one.

The Role of BIN1

The membrane curvature and tubule-forming protein BIN1 is involved in t-tubule biogenesis in both skeletal and cardiac muscle (89) and is known to play a role in targeted delivery of $Ca_V1.2$ LTCCs to t-tubules (90). A cardiac-specific isoform of BIN1 (BIN1+13+17) has been linked with the formation of microfolds on t-tubules (91). These BIN1-scaffolded microfolds limit ionic diffusion within t-tubules, which may allow efficient recapture of extruded Ca^{2+} (90). Cardiac-specific heterozygous KO of BIN1 lowers capacitance of cardiomyocytes due to the reduced amount of t-tubule membrane (90). The microfolds are also thought to facilitate the formation of dyadic microdomains, as BIN1 delivers $Ca_V1.2$ channels to these t-tubule folds via microtubules, and jSR-localized RyR2 channels are proposed to be attracted to these sites (92). Accordingly, super-resolution stochastic optical reconstruction microscopy or STORM imaging has revealed close associations between $Ca_V1.2$, RyR2, and BIN1 in adult mouse cardiomyocytes (92). Thus, if BIN1 levels are downregulated, and fewer microfolds are formed, one may expect there to be fewer interfaces for dyad formation.

BIN1 is also downregulated in heart failure (87, 90), and this has been linked to pathogenesis because cardiac-specific KO of BIN1 precipitates dilated cardiomyopathy in mice (90). Interestingly, in sheep and ferret models of heart failure, reduced t-tubule density occurs coincident with decreased BIN1 expression, and these alterations occur in the absence of any change in JPH2 expression (87). BIN1 knockdown in adult rat ventricular myocytes leads to reduced t-tubule density and increased Ca^{2+} transient dyssynchrony, suggesting disrupted dyads and altered Ca^{2+} signaling, whereas JPH2 knockdown leads to more longitudinally arranged t-tubules but not a change in overall density (87).

Lentiviral transduction of BIN1 in human embryonic stem cell–derived cardiomyocytes results in membrane tubulation and $Ca_V1.2$ cluster recruitment to those tubules to form functional Ca^{2+} release unit microdomains containing $Ca_V1.2$-RyR2 (93). Virally mediated BIN1 overexpression can restore t-tubule microfolding and normalize $Ca_V1.2$ and RyR2 organization, leading to decreased mortality in a mouse transverse aortic constriction model of pressure-overload-induced heart failure (94). BIN1 expression is reportedly normalized upon delivery of AAV9-SERCA2a in failing, postinfarction rat hearts (95). This treatment rescued t-tubule density and improved Ca^{2+} spark synchronicity, but interestingly, it did not rescue JPH2 levels, implying that BIN1 but not JPH2 is required to maintain a functional t-tubule network and efficient E-C coupling. Taken together, these studies imply a role for BIN1 in t-tubule biogenesis and maintenance and in the recruitment and retention of $Ca_V1.2$ on t-tubules. Loss of BIN1 destabilizes t-tubules and impacts dyad integrity and E-C coupling.

The Role of Nexilin

Nexilin (NEXN) is an actin-binding and z-disk-stabilizing protein (96, 97) recently identified as a critical determinant of dyad formation and stability. Mutations or genetic ablation of NEXN are associated with cardiomyopathy in zebrafish, mice, and humans (97–101). Global KO of NEXN is associated with perinatal lethality, with mice succumbing to dilated cardiomyopathy within 8 days of birth (100), while cardiac-specific KO also precipitated dilated cardiomyopathy and lethality within 12 days (102). In the cardiac-specific KO model, loss of NEXN led to reduced expression of other dyadic proteins, including $Ca_V1.2$, RyR2, and JPH2, whereas BIN1 expression was unaltered (102). NEXN colocalizes and copurifies with JPH2 and RyR2, confirming NEXN as a dyad-localized protein, and EM studies of cardiac-specific NEXN KO myocytes revealed a significant reduction in the number of ∼12-nm SR-PM junctions, suggesting NEXN's critical role in dyad formation and integrity. Furthermore, t-tubules fail to form in cardiac-specific NEXN KO mice, suggesting an essential role in t-tubule formation. The mice likely survive the first 12 days after birth as peripheral couplings (∼30-nm junctional distance) between surface sarcolemma and SR still form to sustain a low but ultimately inadequate level of E-C coupling (102). Inducible KO of NEXN in adult cardiomyocytes also precipitated dilated cardiomyopathy and led to altered Ca^{2+} handling and t-tubule network remodeling (98). Together, these studies suggest that NEXN is involved in t-tubule biogenesis, maintenance, and regulation, although the exact mechanism by which NEXN, BIN1, and JPH2 function together to exert their effects, including how they influence expression of other dyadic proteins, remains unknown.

SMOOTH MUSCLE SARCOPLASMIC RETICULUM–PLASMA MEMBRANE JUNCTIONS

SMCs that line blood vessels, airways, and the gastrointestinal, urinary, and reproductive tracts are significantly thinner and smaller than their striated muscle counterparts and thus do not require a complex, penetrating network of t-tubules to ensure uniform conduction of electrical depolarizations. Instead, SMCs have many shallow, caveolin-scaffolded, flask-shaped invaginations of their PM, termed caveolae (103). Junctional membrane complexes called peripheral couplings form at interfaces between the caveolar PM or the surface PM and the underlying peripheral SR (103, 104). The reported distance between the two membranes at these points representing SR-PM junctions in SMCs ranges from 10 to 20 nm (104). Peripheral couplings have been implicated in force generation in visceral and vascular smooth muscle tissues. SMC peripheral couplings are sites of BK channel–RyR2 cross talk that play an important role in regulating SMC contractility (105, 106). In vascular SMCs (VSMCs), functional coupling between BK and RyR2 generates a spontaneous transient outward current. This results in membrane hyperpolarization in response to elevated cytosolic Ca^{2+} levels that can occur downstream of depolarization-induced opening of LTCCs, thus favoring vasodilation of blood vessels (**Figure 1*c***, **subpanel *i***). A similar cross talk between these channels is associated with SMC relaxation in phasic smooth muscle tissues, including that of the bladder (107).

PM-localized TRPM4 (transient receptor potential melastatin 4) and SR-localized inositol 1,4,5-trisphosphate (IP_3) receptors (IP_3Rs) are also functionally coupled at peripheral coupling sites in VSMCs (108). In this case, the release of Ca^{2+} from IP_3Rs activates TRPM4 channels that conduct Na^+ into the cells, depolarizing the membrane and favoring the opening of LTCCs and consequent vasoconstriction (108, 109) (**Figure 1*c***, **subpanel *ii***). Finally, in some smooth muscle tissues, RyR- or IP_3R-mediated Ca^{2+} release triggers the opening of Ca^{2+}-activated Cl^- channels that generate a spontaneous transient inward current that depolarizes the muscle and favors contraction (110) (**Figure 1*c***, **subpanel *iii***).

PERIPHERAL COUPLING FORMATION AND MAINTENANCE

There remains a scarcity of information on how and when peripheral couplings are formed in SMCs, but recent work has provided some insight into how they are supported and maintained. In cerebral artery SMCs, peripheral couplings are supported by microtubule arches that press the SR against the PM (111). The microtubule-depolymerizing agent nocodazole is reported to increase SR-PM distances in cerebral artery SMCs up to fourfold, while actin depolymerization had no appreciable effect in diffraction-limited confocal microscopy (111). Furthermore, in superresolution imaging experiments with 20–30-nm lateral resolution, nocodazole significantly reduced the colocalization between SR-localized RyR2 and PM-localized BK channels. As discussed above, these two channels functionally couple to one another to orchestrate SMC relaxation in response to elevations in intracellular Ca^{2+} concentration. This coupling is reliant on the nanometer proximity between the two within peripheral coupling signaling microdomains. Accordingly, nocodazole treatment was seen to alter the kinetic and spatial properties of Ca^{2+} sparks, reducing BK channel activity and promoting hypercontractility, as evidenced by a higher myogenic tone of pressurized artery preparations (111). Several proteins have been found to support and tether peripheral couplings. Here, we consider the roles of junctophilin and STIM1.

The Role of Junctophilin 2

Although less widely studied in SMCs compared to striated muscle, recent work has revealed an important role for JPH2 in regulating the membrane potential and contractile activity of vascular smooth muscle, in that morpholino-mediated JPH2 silencing reduced the number of SR-PM peripheral coupling sites (112). At these sites, JPH2 colocalizes with RyR2, and although JPH2 knockdown does not appear to alter Ca^{2+} spark generation or morphology, it leads to reduced BK channel activity and hypercontractility. Silencing of JPH2 with siRNA has been independently shown to reduce BK channel activity in rat mesenteric arteries (113), where JPH2 is postulated to form a macromolecular complex with BK channels, RyR1, and caveolin-1 (Cav-1). A direct association between Cav-1 and JPH2 has been isolated to a 20-aa sequence on JPH2, and Cav-1-null mice display reduced JPH2-BK channel colocalization. This indicates that Cav-1 recruits BK channels to JPH2-tethered caveolar peripheral couplings, permitting their efficient functional interactions with RyR2 (113, 114). Together, this evidence suggests an essential role for JPH2 in tethering and maintaining peripheral coupling sites to ensure adequate proximity between SR RyR2 and PM BK channels for regulation of SMC contractility.

The Role of STIM1

A recent study found that STIM1 was constitutively active and played an unconventional role in VSMCs, acting independently of Orai1 and SOCE to stabilize peripheral coupling sites (115). Smooth muscle–specific, inducible STIM1 KO mice have been observed to possess fewer and smaller peripheral coupling sites and reduced RyR2-BK channel colocalization. TRPM4:IP_3 SR-PM sites are also impacted by STIM1 KO and, thus, the balance between contractile and dilatory pathways is altered (115). Ultimately, the animals are hypotensive, suggesting impaired contractility of the VSMCs. Superresolution microscopy also hints that SR-anchored STIM1 may interact with BK channels and TRPM4 channels on the PM (115), and although this remains to be confirmed with biochemical approaches, it could provide some mechanistic insight into how STIM1 stabilizes these specific sites.

ENDOPLASMIC RETICULUM–PLASMA MEMBRANE JUNCTIONS IN NEURONS

Shortly after the discovery of ER-PM junctions in striated muscle, EM images from neurons revealed a distinct form of ER-PM junctions named subsurface cisternae in which stacks of ER cisterns were found in close apposition to PM (116, 117). It was noted soon after that the structure of the junction between the most PM-proximal ER cistern and PM in neurons was similar to junctional triads of skeletal muscle (118), with a 10–20-nm gap between ER and PM filled with electron-dense material. Presumably this electron-dense material represents proteins that form the physical structure that maintains close apposition of ER and PM at these sites, together with signaling proteins that mediate the functions associated with these specialized microdomains. However, a comprehensive analysis of components of neuronal ER-PM junctions is for the most part lacking. Detailed morphometric ultrastructural analyses reveal that brain neurons have extensive portions of PM engaged in ER-PM junctions (119), especially on their cell bodies or somata, with certain neurons having >12% of their somatic PM surface area engaged in an ER-PM junction (119). Given the cellular and molecular complexity of the brain (120), it is not surprising that many of the proteins that contribute to the formation and maintenance of ER-PM junctions in other mammalian cell types (2, 3) are also expressed in the brain, at least at the messenger RNA (mRNA) level. In most cases, their expression and localization at neuronal ER-PM junctions or their contribution to depolarization-induced Ca^{2+} signaling has not been defined, but recent studies have provided numerous cases showing the contributions of junction-forming proteins and specific classes of ER-PM junctions to this important form of neuronal Ca^{2+} signaling.

Depolarization-Induced Ca^{2+} Signaling Events at Neuronal Endoplasmic Reticulum–Plasma Membrane Junctions

Neurons have many different forms of Ca^{2+} signaling, including the form triggered by membrane depolarization (121). As in cardiomyocytes, Ca^{2+} influx through PM voltage-gated Ca^{2+} channels (VGCCs) can trigger CICR in neurons, with Ca^{2+} sparks observed in somata and proximal dendrites of hippocampal pyramidal neurons (122–125) at sites in close spatial proximity to PM (125–127). Applying selective inhibitors of LTCCs or RyRs blocks these spontaneous Ca^{2+} sparks (122–125). RyRs are present in high-density clusters at ER-PM junctions containing high-density clusters of the junction-forming voltage-gated $K_V2.1$ K^+ channel protein, such as striatal medium spiny and thalamic neurons (128) and hippocampal pyramidal neurons (42, 125, 129, 130). In somata of cultured hippocampal neurons these sites also contain clustered LTCCs and represent hot spots for Ca^{2+} sparks (125) (**Figure 2*a***).

Owing to their relatively low affinity for Ca^{2+}, BK channels must localize near their Ca^{2+} source for reliable Ca^{2+}-dependent activation (131), and in certain neurons they are localized at neuronal ER-PM junctions. In cartwheel interneurons of the dorsal cochlear nucleus, RyR-mediated ER Ca^{2+} release triggered by PM $Ca_V2.1$ channels activates somatic BK channels (127). $Ca_V2.1$ Ca^{2+} channels and BK channels also colocalize over somatic subsurface cisternae in cerebellar Purkinje cells (132), indicating that these $Ca_V2.1$-RyR-BK triads are present at ER-PM junctions (**Figure 2*b***). In neurons of the suprachiasmatic nucleus, BK channels exhibit a circadian dependence in activation by PM LTCCs (day) or ER RyRs (night) (133). It is intriguing that this diurnal switch in Ca^{2+} sources could represent dynamic changes in BK channel localization at ER-PM junctions.

Another form of CICR are Ca^{2+} puffs (124) resulting from Ca^{2+}-dependent activation of Ca^{2+} release from ER IP_3Rs (134, 135). In hippocampal neurons Ca^{2+} puffs occur on the soma and the

major apical dendrite but not on oblique branches that contain the bulk of dendritic spines (124). Although the sites of Ca^{2+} puffs correspond to prominent sites of ER-PM junctions in neurons (119), whether this localized Ca^{2+} release occurs at neuronal ER-PM junctions has not been determined, but in nonexcitable HeLa cells local IP_3R Ca^{2+} release occurs at ER-PM junctions (136). Following up on earlier studies (137, 138), a detailed immunogold EM study revealed that ER IP_3Rs and PM BK channels are enriched at subsurface cisternae in cerebellar Purkinje neurons (139).

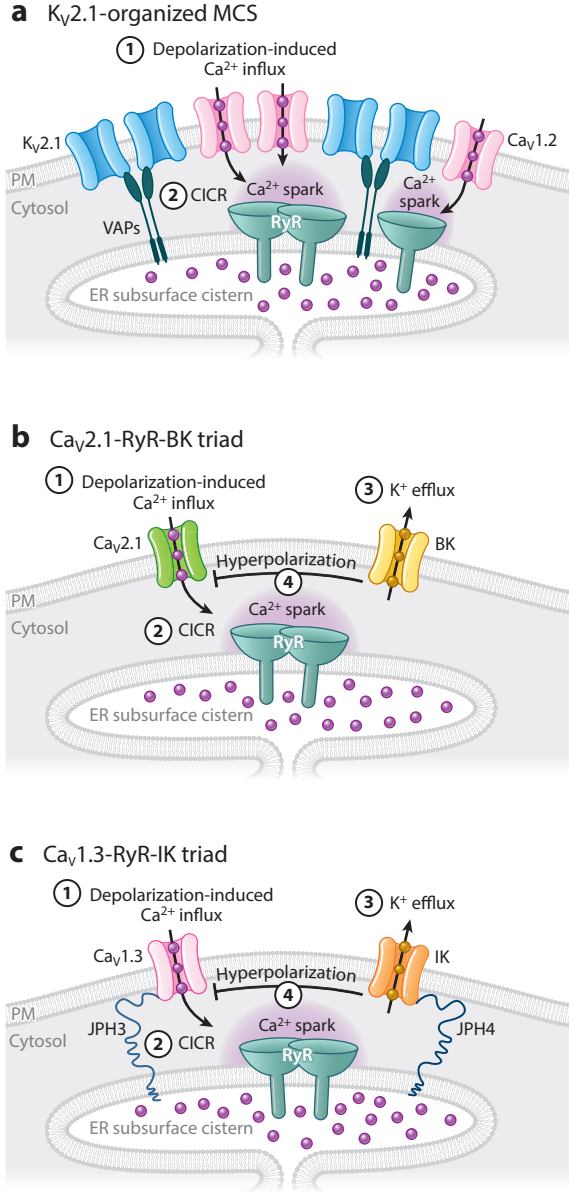

(*Caption appears on following page*)

Figure 2 (*Figure appears on preceding page*)

Neuronal ER-PM junctions as platforms for depolarization-induced Ca^{2+} signaling. (*a*) K_V2-containing ER-PM junctions in hippocampal pyramidal neurons comprise PM $K_V2.1$ (or $K_V2.2$) channels (*blue*) in association with ER VAPs. K_V2 channels recruit PM $Ca_V1.2$ LTCCs (*pink*), leading to their increased clustering that enhances their activity and brings them into close spatial and functional association with ER RyRs (*teal*). The influx of Ca^{2+} (*purple spheres*) through $Ca_V1.2$ ① facilitates depolarization-induced CICR ② and downstream Ca^{2+} signaling pathways, including excitation-transcription coupling. (*b*) PM $Ca_V2.1$ voltage-gated Ca^{2+} channels (*green*) are localized at ER-PM junctions in cartwheel interneurons of the dorsal cochlear nucleus, bringing them into close spatial and functional association with ER RyRs (*teal*). The influx of Ca^{2+} through $Ca_V2.1$ ① facilitates depolarization-induced CICR ② that activates ③ Ca^{2+}-activated BK channels (*yellow*) to hyperpolarize the cell ④ to control action potential firing patterns. (*c*) In hippocampal neurons, $Ca_V1.3$ LTCCs (*pink*) are localized at ER-PM junctions stabilized by JPH3 and JPH4 (*dark blue*), bringing them into close spatial and functional association with ER RyRs (*teal*). The influx of Ca^{2+} through $Ca_V1.3$ ① facilitates depolarization-induced CICR ② that activates ③ Ca^{2+}-activated IK channels (*orange*) to generate the slow afterhyperpolarization ④. Abbreviations: CICR, Ca^{2+}-induced Ca^{2+} release; ER, endoplasmic reticulum; ER-PM, endoplasmic reticulum–plasma membrane; IK, intermediate conductance potassium channel; JPH, junctophilin; LTCC, L-type Ca^{2+} channel; MCS, membrane contact site; RyR, ryanodine receptor; VAP, vesicle-associated membrane protein-associated protein.

Cisternal organelles on the axon initial segment are a highly modified form of subsurface cisternae ER-PM junctions (140). These represent sites at which junction-forming K_V2 channels and ER RyRs are clustered (41) and also sites of axo-axonic GABA synapses (140). High-resolution optical Ca^{2+} imaging reveals highly localized hot spots of depolarization-induced Ca^{2+} signaling on the axon initial segment (141), although the spatial relationship of these hot spots to cisternal organelles has not been defined. ER-PM junctions are not present in dendritic spines (142) or presynaptic terminals (119), although up to 1% of PM surface area of certain axons is engaged in MCS with ER (119). Not surprisingly, given the cellular and molecular complexity of brain neurons, numerous molecules that have been linked to the formation and/or maintenance of ER-PM junctions in other cells (1–3) are expressed in brain. However, for the most part, their presence and role in ER-PM junctions in brain neurons and their contribution to depolarization-induced Ca^{2+} signaling have not been elucidated. Recent studies have linked ER-PM junctions containing neuronal JPH isoforms and those containing PM K_V2 K^+ channels to specialized forms of depolarization-induced Ca^{2+} signaling that profoundly impact neuronal physiology.

Junctophilins and Their Relationship to Depolarization-Induced Ca^{2+} Signaling in Neurons

Although the overall roles of the neuronal JPH3 and JPH4 junctophilin isoforms have not been as firmly established as those of the JPH1 and JPH2 forms in striated muscle, numerous studies support their involvement in neuronal Ca^{2+} signaling. At the RNA level, JPH3 and JPH4 exhibit distinct cellular patterns of expression in the brain (143), suggesting that different neurons may have ER-PM junctions populated by different JPH proteins or combinations thereof. JPH3 and JPH4 single KO mice exhibit motor abnormalities (144–146), presumably related to the high levels of expression of JPH3 and JPH4 in cerebellar Purkinje neurons (143). However, JPH3 and JPH4 appear to be somewhat redundant as overall growth, survival, and behavior are much more profoundly impacted in JPH3/JPH4 double KO mice than in single KO mice, with motor deficits the primary behavioral phenotype (146). Trinucleotide repeats within the *JPH3* gene underlie Huntington disease-like 2 (HDL2), a severe neurodegenerative disorder sharing many similarities to Huntington disease (147). Both JPH3 mRNA and protein are reduced in brains from HDL2 patients (145), although both the loss of function of JPH3 protein (145) and expression of

a polyglutamine repeat protein encoded by the antisense strand of the *JPH3* gene (148) have been implicated in the etiology of HDL2.

Studies employing these KO mice indicate that neuronal JPH proteins are crucial to CICR that triggers afterhyperpolarization (AHP) of the membrane potential following an action potential in numerous types of brain neurons. Different forms of AHPs are mediated by distinct Ca^{2+}-activated K^+ channels that play critical roles in regulation and plasticity of neuronal excitability (149, 150), and diverse forms of Ca^{2+} influx, including CICR, are coupled to activation of AHPs (151–153). CA1 hippocampal neurons from JPH3/JPH4 double KO mice had reduced levels of N-methyl-D-aspartate (NMDA) receptor and RyR-dependent AHPs, impaired Schaffer collateral-CA1 long-term potentiation, and also exhibited deficits in hippocampal-dependent learning (152). Cerebellar Purkinje neurons have a $Ca_V2.1$-triggered and RyR-dependent CICR that activates the small conductance K^+ or SK channel–mediated AHP that is reduced in JPH3/JPH4 double KO mice, perhaps contributing to the motor dysfunction in these mice (146). That it is possible to coimmunoprecipitate exogenously expressed ER JPH2 (the cardiac JPH isoform) and PM SK2 channels from heterologous cells (154) suggests the possibility that neuronal JPH isoforms and SK2 channels may physically interact at ER-PM junctions in neurons.

Hippocampal neurons have LTCC- and RyR-mediated CICR that activates intermediate conductance KCa3.1 Ca^{2+}-activated K^+ channels to generate a slow AHP (155). $Ca_V1.3$-RyR2-KCa3.1 exist in a tripartite complex, and superresolution total internal reflection fluorescence (TIRF) imaging shows that these proteins are coclustered with JPH3 and JPH4 at somatic sites that presumably represent ER-PM junctions (**Figure 2*c***). Knockdown experiments show that JPH3 and JPH4 expression is necessary to maintain this tripartite complex and for normal activation of a slow AHP current (155). These results support that CICR at JPH-containing ER-PM junctions regulates different forms of Ca^{2+}-dependent AHPs that impact neuronal action potential firing.

Neuronal JPH3 and JPH4 were capable of inducing clustering of coexpressed Ca_V1 and Ca_V2 Ca^{2+} channels and changes in $Ca_V2.1$ and $Ca_V2.2$ gating (156). When coexpressed, JPH3 colocalized with all three RyR isoforms, RyR1–3, but JPH4 only colocalized with RyR3. The region on $Ca_V1.2$ and $Ca_V1.3$ LTCCs that is required for mediating coclustering with neuronal JPH isoforms appears to be analogous to that mediating the binding of skeletal muscle $Ca_V1.1$ to JPH1 (156). However, Ca_V2 Ca^{2+} channels lack this motif and presumably associate with JPH3 and JPH4 in a distinct manner. These studies suggest that distinct combinations of VGCC, RyR, and JPH isoforms could contribute to depolarization-induced Ca^{2+} signaling in different neurons, or as VGCC isoforms exhibit substantial differences in their subcellular localization (157), in different neuronal compartments. However, the subcellular localization of endogenous JPH isoforms in brain neurons has not been established. As such, their relationship to sites of VGCC and RyR clustering and to the ER-PM junctions that have been defined both anatomically and with molecular markers remains unknown.

$K_V2.1$: VAP Endoplasmic Reticulum–Plasma Membrane Junctions and Their Relationship to Depolarization-Induced Ca^{2+} Signaling in Neurons

K_V2 channels function as voltage-gated K^+ channels regulating neuronal action potential firing (158–160). $K_V2.1$, its paralog $K_V2.2$, and their auxiliary AMIGO-1 subunit are unique among neuronal PM proteins in being present in large clusters on somata, proximal dendrites, and the axon initial segment (161–163) that represent ER-PM junctions (42, 128, 129, 164). A detailed morphometric analysis in hippocampal CA1 pyramidal neurons showed that more than 90% of subsurface cisternae encountered were positive for $K_V2.1$ immunogold labeling (164), suggesting that K_V2

channels, which have a broad expression throughout the mammalian brain (165), may broadly contribute to the organization of somatic ER-PM junctions that are so prominent in brain neurons (119). K_V2 channels function to organize ER-PM junctions (166–168) as a nonconducting (i.e., physical) function (168). Mass spectrometry–based proteomic analyses employing either proximity biotinylation in transfected cells exogenously expressing $K_V2.1$ (167) or immunopurification of native $K_V2.1$ complexes from cross-linked mouse brain samples (42) led to the identification of VAPs as the ER proteins associated with PM $K_V2.1$. Binding to VAPs is mediated by the PRC domain on the long C-terminal tail of K_V2 channels (42, 167). The proximal restriction and clustering or PRC domain is necessary and sufficient for K_V2-like clustering on neuronal somata (169) and is widely used to effectively direct somatic localization of optogenetic reporters (170). VAPs interact with a variety of cytoplasmic proteins, referred to as the VAPome, localizing them to ER (171). The cytoplasmic MSP domain of VAPs binds to two phenylalanines in an acidic tract (FFAT) motifs, and the $K_V2.1$ PRC represents a noncanonical FFAT motif (42, 167) whose acidic nature is provided by PRC domain phosphoserine residues defined in phosphoproteomics studies (172) and whose mutation eliminates $K_V2.1$ clustering (169). Changes in phosphorylation at these sites represent the molecular mechanism of activity-dependent, phosphorylation-dependent regulation of $K_V2.1$ clustering (125, 173). Ancient forms of metazoan K_V2 channels function as voltage-gated ion channels but lack a PRC domain (174), such that their nonconducting function to bind VAPs and organize ER-PM junctions is a later acquisition than their canonical roles as K^+ channels.

$K_V2.1$-containing ER-PM junctions (**Figure 2*a***) are enriched in Ca^{2+} signaling proteins including PM LTCC subunits, ER RyRs, calcineurin and others (125). In heterologous cells and hippocampal neurons, activity of $Ca_V1.2$ LTCCs is enhanced by its clustering at $K_V2.1$-containing ER-PM junctions (125), at least in part through the cooperative gating mechanism described above. A recent study in VSMCs shows that $K_V2.1$ similarly promotes the clustering and enhanced activity of $Ca_V1.2$ LTCCs to amplify Ca^{2+} influx resulting in increased vasoconstriction (175). As in neurons, $K_V2.1$ also contributes to VSMC Ca^{2+} signaling through its action as a K^+ channel, hyperpolarizing the cells and thus opposing vasoconstriction (176).

In hippocampal neurons, $K_V2.1$-containing ER-PM junctions represent hot spots for LTCC-mediated CICR on neuronal somata, and cells lacking $K_V2.1$ expression have reduced spatial and functional association of LTCCs and RyRs and spontaneous Ca^{2+} spark frequency (125). Dynamically altering $K_V2.1$ clustering by treatments that bidirectionally modulate phosphorylation-dependent binding of $K_V2.1$ to VAP proteins yields parallel changes in LTCC activity and the extent of their association with RyRs (125). The $K_V2.1$ C terminus also contains a separate Ca^{2+} channel association domain motif that is necessary and sufficient for recruitment of LTCCs to $K_V2.1$-containing ER-PM junctions (177). A cell-penetrating peptide containing this motif disrupts LTCC clustering at $K_V2.1$-containing ER-PM junctions without altering the junctions themselves. It also leads to reduced LTCC clustering and activity and Ca^{2+} spark frequency, as does coexpression with a $K_V2.1$ mutant with point mutations in the Ca^{2+} channel association domain. Interestingly, disrupting LTCC clustering at $K_V2.1$-containing ER-PM junctions robustly reduced levels of depolarization-induced activation of the transcription factors CREB and c-Fos, suggesting an important role of $K_V2.1$-containing ER-PM junctions on neuronal somata in excitation-transcription coupling (177). The relationship of $K_V2.1$-containing ER-PM junctions to other junction-forming molecules expressed in neurons and to other forms of depolarization-induced Ca^{2+} signaling that occur at these MCS in neurons remains to be elucidated.

CONCLUSIONS AND FUTURE PERSPECTIVES

The studies reviewed above provide numerous examples of the molecular architecture, structure, and function of ER-PM junctions mediating different forms of depolarization-induced Ca^{2+} signaling in excitable cells. However, much future research is still needed to define the molecular composition and functional role of many classes of ER-PM junctions that can be observed microscopically. There exists a tremendous diversity of ER-PM junction structure in excitable cells. As we review here, recent studies have begun to define at molecular and in some cases atomic detail the macromolecular complexes that underlie the depolarization-induced Ca^{2+} signaling events that represent the crucial functions of some of the most well-defined of these junctions (e.g., triads of skeletal muscle and dyads in cardiac muscle) and how they differ between distinct types of excitable cells. However, even in these well-studied tissues there are alternative forms (e.g., those that form with axial tubules and surface sarcolemma in striated muscle) whose molecular composition and functional role are not as defined, a situation that also holds for the peripheral couplings of smooth muscle and the diverse forms of ER-PM junctions in neurons. In neurons, a diversity of structures exist in the cell body alone (119), suggesting differences in molecular composition and function that could provide compartmentalization of PM-associated Ca^{2+} signaling events, as occurs in the specialized structures of dendritic spines and presynaptic terminals, in the otherwise non-compartmentalized PM of the soma.

Another important aspect of ER-PM junctions is their dynamic regulation (178, 179). The molecular mechanisms underlying the interconversion between the different forms of ER-PM junctions seen in static micrographs remain mostly unknown. This also applies to changes during development, with aging, and in response to injury and disease. In dividing cells ER-PM junctions disassemble and rebuild their junctions in a cell cycle–dependent manner (180). Striated muscle cells and neurons are terminally differentiated and, although not subject to this challenge, still need to dynamically regulate ER-PM junctions to meet their own special needs. For example, muscle SR-PM contacts are subjected to mechanical stresses and strains that most cell types, including neurons, do not encounter. Elegant work recently captured some of the effects of these mechanical forces on cardiomyocytes, where t-tubule membranes were seen to be compressed and deformed as cells shortened during a contraction (181). These forces are also likely to be experienced by jSR elements. One can also envisage them being pushed toward t-tubule membranes as the cell contracts and pulls away again as it relaxes and, in the case of myocardium, undergoes stretch during diastolic filling. To survive those repetitive forces, it seems necessary that tethers holding these junctions together should be flexible, numerous, and tough. One can also imagine the large cytosolic domains of RyR2 or IP_3R as bumpers of a sort that may prevent the two membranes from crashing into one another. In smooth muscle, their contractions in the absence of regular sarcomeres would create a scrunching motion of those cells that could wreak havoc on peripheral couplings. Future investigations should examine the effects of these mechanical forces on muscle SR-PM junctions and the consequences of these deformations for E-C coupling and SOCE. Neurons exhibit activity-dependent changes in ER-PM junctions. The number and length of ER-PM junctions in hippocampal neurons are reduced in response to numerous stimuli that increase neuronal activity and cytoplasmic [Ca^{2+}] (182). These same stimuli impact the presence and functional contribution of $K_V2.1$ at ER-PM junctions (125, 173) and those formed by the association of STIM and Orai (22). The junction-forming properties of other ER-PM junction proteins are also regulated by diverse intracellular processes, including changes in PM lipid composition, cytoplasmic [Ca^{2+}], and phosphorylation state. These provide a foundation for mediating the dynamic changes in ER-PM junction structure and function that meet the physiological needs of the cells in which they reside. This is especially true for the Ca^{2+}-dependent mechanisms of

ER-PM junction plasticity that provide dynamic regulation of the crucial depolarization-induced Ca^{2+} signaling that occurs at these sites in excitable cells.

DISCLOSURE STATEMENT

The authors are not aware of any affiliations, memberships, funding, or financial holdings that might be perceived as affecting the objectivity of this review.

ACKNOWLEDGMENTS

Research from our laboratories presented here was supported by the US National Institutes of Health through grants R01AG063796 (R.E.D.) and R01NS114210 and R01HL144071 (J.S.T.).

LITERATURE CITED

1. Prinz WA, Toulmay A, Balla T. 2020. The functional universe of membrane contact sites. *Nat. Rev. Mol. Cell Biol.* 21:7–24
2. Henne WM, Liou J, Emr SD. 2015. Molecular mechanisms of inter-organelle ER-PM contact sites. *Curr. Opin. Cell Biol.* 35:123–30
3. Stefan CJ. 2020. Endoplasmic reticulum-plasma membrane contacts: principals of phosphoinositide and calcium signaling. *Curr. Opin. Cell Biol.* 63:125–34
4. Burgoyne T, Patel S, Eden ER. 2015. Calcium signaling at ER membrane contact sites. *Biochim. Biophys. Acta Mol. Cell Res.* 1853:2012–17
5. Balla T. 2018. Ca^{2+} and lipid signals hold hands at endoplasmic reticulum-plasma membrane contact sites. *J. Physiol.* 596:2709–16
6. Dickson EJ. 2022. Phosphoinositide transport and metabolism at membrane contact sites. *Biochim. Biophys. Acta Mol. Cell Biol. Lipids* 1867:159107
7. Porter KR, Palade GE. 1957. Studies on the endoplasmic reticulum. III. Its form and distribution in striated muscle cells. *J. Biophys. Biochem. Cytol.* 3:269–300
8. Franzini-Armstrong C. 1970. Studies of the triad: I. Structure of the junction in frog twitch fibers. *J. Cell Biol.* 47:488–99
9. Bannister RA, Beam KG. 2013. $Ca_V1.1$: The atypical prototypical voltage-gated Ca^{2+} channel. *Biochim. Biophys. Acta Biomembr.* 1828:1587–97
10. Armstrong CM, Bezanilla FM, Horowicz P. 1972. Twitches in the presence of ethylene glycol bis(β-aminoethyl ether)-*N*,*N*′-tetracetic acid. *Biochim. Biophys. Acta Bioenerg.* 267:605–8
11. Gonzalez-Serratos H, Valle-Aguilera R, Lathrop DA, Garcia MC. 1982. Slow inward calcium currents have no obvious role in muscle excitation-contraction coupling. *Nature* 298:292–94
12. Nakai J, Dirksen RT, Nguyen HT, Pessah IN, Beam KG, Allen PD. 1996. Enhanced dihydropyridine receptor channel activity in the presence of ryanodine receptor. *Nature* 380:72–75
13. Dirksen RT, Beam KG. 1999. Role of calcium permeation in dihydropyridine receptor function. Insights into channel gating and excitation-contraction coupling. *J. Gen. Physiol.* 114:393–403
14. Polster A, Perni S, Filipova D, Moua O, Ohrtman JD, et al. 2018. Junctional trafficking and restoration of retrograde signaling by the cytoplasmic RyR1 domain. *J. Gen. Physiol.* 150:293–306
15. Avila G, Dirksen RT. 2000. Functional impact of the ryanodine receptor on the skeletal muscle L-type Ca^{2+} channel. *J. Gen. Physiol.* 115:467–80
16. Franzini-Armstrong C, Pincon-Raymond M, Rieger F. 1991. Muscle fibers from dysgenic mouse in vivo lack a surface component of peripheral couplings. *Dev. Biol.* 146:364–76
17. Takekura H, Nishi M, Noda T, Takeshima H, Franzini-Armstrong C. 1995. Abnormal junctions between surface membrane and sarcoplasmic reticulum in skeletal muscle with a mutation targeted to the ryanodine receptor. *PNAS* 92:3381–85
18. Samso M. 2017. A guide to the 3D structure of the ryanodine receptor type 1 by cryoEM. *Protein Sci.* 26:52–68

19. Yan Z, Bai X, Yan C, Wu J, Li Z, et al. 2015. Structure of the rabbit ryanodine receptor RyR1 at near-atomic resolution. *Nature* 517:50–55
20. Block BA, Imagawa T, Campbell KP, Franzini-Armstrong C. 1988. Structural evidence for direct interaction between the molecular components of the transverse tubule/sarcoplasmic reticulum junction in skeletal muscle. *J. Cell Biol.* 107:2587–600
21. Di Biase V, Franzini-Armstrong C. 2005. Evolution of skeletal type e–c coupling: a novel means of controlling calcium delivery. *J. Cell Biol.* 171:695–704
22. Emrich SM, Yoast RE, Trebak M. 2022. Physiological functions of CRAC channels. *Annu. Rev. Physiol.* 84:355–79
23. Prakriya M, Lewis RS. 2015. Store-operated calcium channels. *Physiol. Rev.* 95:1383–436
24. Lewis RS. 2020. Store-operated calcium channels: from function to structure and back again. *Cold Spring Harb. Perspect. Biol.* 12:a035055
25. Michelucci A, Garcia-Castaneda M, Boncompagni S, Dirksen RT. 2018. Role of STIM1/ORAI1-mediated store-operated Ca^{2+} entry in skeletal muscle physiology and disease. *Cell Calcium* 76:101–15
26. Takeshima H, Shimuta M, Komazaki S, Ohmi K, Nishi M, et al. 1998. Mitsugumin29, a novel synaptophysin family member from the triad junction in skeletal muscle. *Biochem. J.* 331(Part 1):317–22
27. Betz H, Becker CM, Grenningloh G, Hoch W, Knaus P, et al. 1989. Homology and analogy in transmembrane channel design: lessons from synaptic membrane proteins. *J. Protein Chem.* 8:325
28. Chang CW, Hsiao YT, Jackson MB. 2021. Synaptophysin regulates fusion pores and exocytosis mode in chromaffin cells. *J. Neurosci.* 41:3563–78
29. Komazaki S, Nishi M, Kangawa K, Takeshima H. 1999. Immunolocalization of mitsugumin29 in developing skeletal muscle and effects of the protein expressed in amphibian embryonic cells. *Dev. Dyn.* 215:87–95
30. Nishi M, Komazaki S, Kurebayashi N, Ogawa Y, Noda T, et al. 1999. Abnormal features in skeletal muscle from mice lacking mitsugumin29. *J. Cell Biol.* 147:1473–80
31. Takeshima H, Komazaki S, Nishi M, Iino M, Kangawa K. 2000. Junctophilins: a novel family of junctional membrane complex proteins. *Mol. Cell* 6:11–22
32. Garbino A, van Oort RJ, Dixit SS, Landstrom AP, Ackerman MJ, Wehrens XH. 2009. Molecular evolution of the junctophilin gene family. *Physiol. Genom.* 37:175–86
33. Bennett HJ, Davenport JB, Collins RF, Trafford AW, Pinali C, Kitmitto A. 2013. Human junctophilin-2 undergoes a structural rearrangement upon binding PtdIns(3,4,5)P_3 and the S101R mutation identified in hypertrophic cardiomyopathy obviates this response. *Biochem. J.* 456:205–17
34. Rossi D, Scarcella AM, Liguori E, Lorenzini S, Pierantozzi E, et al. 2019. Molecular determinants of homo- and heteromeric interactions of Junctophilin-1 at triads in adult skeletal muscle fibers. *PNAS* 116:15716–24
35. Yang ZF, Panwar P, McFarlane CR, Tuinte WE, Campiglio M, Van Petegem F. 2022. Structures of the junctophilin/voltage-gated calcium channel interface reveal hot spot for cardiomyopathy mutations. *PNAS* 119:e2120416119
36. Jiang M, Hu J, White FKH, Williamson J, Klymchenko AS, et al. 2019. *S*-Palmitoylation of junctophilin-2 is critical for its role in tethering the sarcoplasmic reticulum to the plasma membrane. *J. Biol. Chem.* 294:13487–501
37. Ito K, Komazaki S, Sasamoto K, Yoshida M, Nishi M, et al. 2001. Deficiency of triad junction and contraction in mutant skeletal muscle lacking junctophilin type 1. *J. Cell Biol.* 154:1059–67
38. Komazaki S, Ito K, Takeshima H, Nakamura H. 2002. Deficiency of triad formation in developing skeletal muscle cells lacking junctophilin type 1. *FEBS Lett.* 524:225–29
39. Hirata Y, Brotto M, Weisleder N, Chu Y, Lin P, et al. 2006. Uncoupling store-operated Ca^{2+} entry and altered Ca^{2+} release from sarcoplasmic reticulum through silencing of junctophilin genes. *Biophys. J.* 90:4418–27

40. Guarina L, Moghbel AN, Pourhosseinzadeh MS, Cudmore RH, Sato D, et al. 2022. Biological noise is a key determinant of the reproducibility and adaptability of cardiac pacemaking and EC coupling. *J. Gen. Physiol.* 154:e202012613
41. King AN, Manning CF, Trimmer JS. 2014. A unique ion channel clustering domain on the axon initial segment of mammalian neurons. *J. Comp. Neurol.* 522:2594–608
42. Kirmiz M, Vierra NC, Palacio S, Trimmer JS. 2018. Identification of VAPA and VAPB as Kv2 channel-interacting proteins defining endoplasmic reticulum-plasma membrane junctions in mammalian brain neurons. *J. Neurosci.* 38:7562–84
43. Golini L, Chouabe C, Berthier C, Cusimano V, Fornaro M, et al. 2011. Junctophilin 1 and 2 proteins interact with the L-type Ca^{2+} channel dihydropyridine receptors (DHPRs) in skeletal muscle. *J. Biol. Chem.* 286:43717–25
44. Nakada T, Kashihara T, Komatsu M, Kojima K, Takeshita T, Yamada M. 2018. Physical interaction of junctophilin and the $Ca_V1.1$ C terminus is crucial for skeletal muscle contraction. *PNAS* 115:4507–12
45. Phimister AJ, Lango J, Lee EH, Ernst-Russell MA, Takeshima H, et al. 2007. Conformation-dependent stability of junctophilin 1 (JP1) and ryanodine receptor type 1 (RyR1) channel complex is mediated by their hyper-reactive thiols. *J. Biol. Chem.* 282:8667–77
46. Rufenach B, Van Petegem F. 2021. Structure and function of STAC proteins: calcium channel modulators and critical components of muscle excitation-contraction coupling. *J. Biol. Chem.* 297:100874
47. Shishmarev D. 2020. Excitation-contraction coupling in skeletal muscle: recent progress and unanswered questions. *Biophys. Rev.* 12:143–53
48. Perni S, Lavorato M, Beam KG. 2017. De novo reconstitution reveals the proteins required for skeletal muscle voltage-induced Ca^{2+} release. *PNAS* 114:13822–27
49. Di Maio A, Karko K, Snopko RM, Mejia-Alvarez R, Franzini-Armstrong C. 2007. T-tubule formation in cardiacmyocytes: Two possible mechanisms? *J. Muscle Res. Cell Motil.* 28:231–41
50. Pinali C, Bennett H, Davenport JB, Trafford AW, Kitmitto A. 2013. Three-dimensional reconstruction of cardiac sarcoplasmic reticulum reveals a continuous network linking transverse-tubules: this organization is perturbed in heart failure. *Circ. Res.* 113:1219–30
51. Shiels HA, Galli GL. 2014. The sarcoplasmic reticulum and the evolution of the vertebrate heart. *Physiology* 29:456–69
52. Kawai M, Hussain M, Orchard CH. 1999. Excitation-contraction coupling in rat ventricular myocytes after formamide-induced detubulation. *Am. J. Physiol.* 277:H603–9
53. Del Villar SG, Voelker TL, Westhoff M, Reddy GR, Spooner HC, et al. 2021. β-Adrenergic control of sarcolemmal $Ca_V1.2$ abundance by small GTPase Rab proteins. *PNAS* 118:e2017937118
54. Ito DW, Hannigan KI, Ghosh D, Xu B, Del Villar SG, et al. 2019. β-Adrenergic-mediated dynamic augmentation of sarcolemmal $Ca_V1.2$ clustering and co-operativity in ventricular myocytes. *J. Physiol.* 597:2139–62
55. Dixon RE, Moreno CM, Yuan C, Opitz-Araya X, Binder MD, et al. 2015. Graded Ca^{2+}/calmodulin-dependent coupling of voltage-gated $Ca_V1.2$ channels. *eLife* 4:e05608
56. Scriven DR, Asghari P, Schulson MN, Moore ED. 2010. Analysis of $Ca_V1.2$ and ryanodine receptor clusters in rat ventricular myocytes. *Biophys. J.* 99:3923–29
57. Cheng H, Lederer WJ. 2008. Calcium sparks. *Physiol. Rev.* 88:1491–545
58. Tanskanen AJ, Greenstein JL, Chen A, Sun SX, Winslow RL. 2007. Protein geometry and placement in the cardiac dyad influence macroscopic properties of calcium-induced calcium release. *Biophys. J.* 92:3379–96
59. Franzini-Armstrong C, Protasi F, Ramesh V. 1999. Shape, size, and distribution of Ca^{2+} release units and couplons in skeletal and cardiac muscles. *Biophys. J.* 77:1528–39
60. Dixon RE. 2021. Nanoscale organization, regulation, and dynamic reorganization of cardiac calcium channels. *Front. Physiol.* 12:810408
61. Wang MC, Collins RF, Ford RC, Berrow NS, Dolphin AC, Kitmitto A. 2004. The three-dimensional structure of the cardiac L-type voltage-gated calcium channel: comparison with the skeletal muscle form reveals a common architectural motif. *J. Biol. Chem.* 279:7159–68
62. Inoue M, Bridge JH. 2003. Ca^{2+} sparks in rabbit ventricular myocytes evoked by action potentials: involvement of clusters of L-type Ca^{2+} channels. *Circ. Res.* 92:532–38

63. Bers DM, Stiffel VM. 1993. Ratio of ryanodine to dihydropyridine receptors in cardiac and skeletal muscle and implications for E-C coupling. *Am. J. Physiol.* 264:C1587–93
64. Quayle JM, McCarron JG, Asbury JR, Nelson MT. 1993. Single calcium channels in resistance-sized cerebral arteries from rats. *Am. J. Physiol.* 264:H470–78
65. Dixon RE, Yuan C, Cheng EP, Navedo MF, Santana LF. 2012. Ca^{2+} signaling amplification by oligomerization of L-type $Ca_V1.2$ channels. *PNAS* 109:1749–54
66. Dixon RE, Navedo MF, Binder MD, Santana LF. 2022. Mechanisms and physiological implications of cooperative gating of clustered ion channels. *Physiol. Rev.* 102:1159–210
67. Ziman AP, Gomez-Viquez NL, Bloch RJ, Lederer WJ. 2010. Excitation-contraction coupling changes during postnatal cardiac development. *J. Mol. Cell. Cardiol.* 48:379–86
68. Kim HD, Kim DJ, Lee IJ, Rah BJ, Sawa Y, Schaper J. 1992. Human fetal heart development after mid-term: morphometry and ultrastructural study. *J. Mol. Cell. Cardiol.* 24:949–65
69. Jones PP, MacQuaide N, Louch WE. 2018. Dyadic plasticity in cardiomyocytes. *Front. Physiol.* 9:1773
70. Drum BM, Yuan C, de la Mata A, Grainger N, Santana LF. 2020. Junctional sarcoplasmic reticulum motility in adult mouse ventricular myocytes. *Am. J. Physiol. Cell Physiol.* 318:C598–604
71. Vega AL, Yuan C, Votaw VS, Santana LF. 2011. Dynamic changes in sarcoplasmic reticulum structure in ventricular myocytes. *J. Biomed. Biotechnol.* 2011:382586
72. Parton RG, Way M, Zorzi N, Stang E. 1997. Caveolin-3 associates with developing T-tubules during muscle differentiation. *J. Cell Biol.* 136:137–54
73. Bryant SM, Kong CHT, Watson JJ, Gadeberg HC, Roth DM, et al. 2018. Caveolin-3 KO disrupts t-tubule structure and decreases t-tubular I_{Ca} density in mouse ventricular myocytes. *Am. J. Physiol. Heart Circ. Physiol.* 315:H1101–11
74. Lehnart SE, Wehrens XHT. 2022. The role of junctophilin proteins in cellular function. *Physiol. Rev.* 102:1211–61
75. Van Oort RJ, Garbino A, Wang W, Dixit SS, Landstrom AP, et al. 2011. Disrupted junctional membrane complexes and hyperactive ryanodine receptors after acute junctophilin knockdown in mice. *Circulation* 123:979–88
76. Munro ML, Jayasinghe ID, Wang Q, Quick A, Wang W, et al. 2016. Junctophilin-2 in the nanoscale organisation and functional signalling of ryanodine receptor clusters in cardiomyocytes. *J. Cell Sci.* 129:4388–98
77. Gross P, Johnson J, Romero CM, Eaton DM, Poulet C, et al. 2021. Interaction of the joining region in junctophilin-2 with the L-type Ca^{2+} channel is pivotal for cardiac dyad assembly and intracellular Ca^{2+} dynamics. *Circ. Res.* 128:92–114
78. Poulet C, Sanchez-Alonso J, Swiatlowska P, Mouy F, Lucarelli C, et al. 2021. Junctophilin-2 tethers T-tubules and recruits functional L-type calcium channels to lipid rafts in adult cardiomyocytes. *Cardiovasc. Res.* 117:149–61
79. Wei S, Guo A, Chen B, Kutschke W, Xie YP, et al. 2010. T-tubule remodeling during transition from hypertrophy to heart failure. *Circ. Res.* 107:520–31
80. Reynolds JO, Chiang DY, Wang W, Beavers DL, Dixit SS, et al. 2013. Junctophilin-2 is necessary for T-tubule maturation during mouse heart development. *Cardiovasc. Res.* 100:44–53
81. Chen B, Guo A, Zhang C, Chen R, Zhu Y, et al. 2013. Critical roles of junctophilin-2 in T-tubule and excitation-contraction coupling maturation during postnatal development. *Cardiovasc. Res.* 100:54–62
82. Landstrom AP, Weisleder N, Batalden KB, Bos JM, Tester DJ, et al. 2007. Mutations in *JPH2*-encoded junctophilin-2 associated with hypertrophic cardiomyopathy in humans. *J. Mol. Cell. Cardiol.* 42:1026–35
83. Zhang HB, Li RC, Xu M, Xu SM, Lai YS, et al. 2013. Ultrastructural uncoupling between T-tubules and sarcoplasmic reticulum in human heart failure. *Cardiovasc. Res.* 98:269–76
84. Guo A, Hall D, Zhang C, Peng T, Miller JD, et al. 2015. Molecular determinants of calpain-dependent cleavage of junctophilin-2 protein in cardiomyocytes. *J. Biol. Chem.* 290:17946–55
85. Matsushita Y, Furukawa T, Kasanuki H, Nishibatake M, Kurihara Y, et al. 2007. Mutation of junctophilin type 2 associated with hypertrophic cardiomyopathy. *J. Hum. Genet.* 52:543–48
86. Reynolds JO, Quick AP, Wang Q, Beavers DL, Philippen LE, et al. 2016. Junctophilin-2 gene therapy rescues heart failure by normalizing RyR2-mediated Ca^{2+} release. *Int. J. Cardiol.* 225:371–80

87. Caldwell JL, Smith CE, Taylor RF, Kitmitto A, Eisner DA, et al. 2014. Dependence of cardiac transverse tubules on the BAR domain protein amphiphysin II (BIN-1). *Circ. Res.* 115:986–96
88. Hou Y, Bai J, Shen X, de Langen O, Li A, et al. 2021. Nanoscale organisation of ryanodine receptors and Junctophilin-2 in the failing human heart. *Front. Physiol.* 12:724372
89. Lee E, Marcucci M, Daniell L, Pypaert M, Weisz OA, et al. 2002. Amphiphysin 2 (Bin1) and T-tubule biogenesis in muscle. *Science* 297:1193–96
90. Hong TT, Smyth JW, Chu KY, Vogan JM, Fong TS, et al. 2012. BIN1 is reduced and Cav1.2 trafficking is impaired in human failing cardiomyocytes. *Heart Rhythm* 9:812–20
91. Hong T, Yang H, Zhang SS, Cho HC, Kalashnikova M, et al. 2014. Cardiac BIN1 folds T-tubule membrane, controlling ion flux and limiting arrhythmia. *Nat. Med.* 20:624–32
92. Fu Y, Shaw SA, Naami R, Vuong CL, Basheer WA, et al. 2016. Isoproterenol promotes rapid ryanodine receptor movement to bridging integrator 1 (BIN1)-organized dyads. *Circulation* 133:388–97
93. De La Mata A, Tajada S, O'Dwyer S, Matsumoto C, Dixon RE, et al. 2019. BIN1 induces the formation of T-tubules and adult-like Ca^{2+} release units in developing cardiomyocytes. *Stem Cells* 37:54–64
94. Li J, Agvanian S, Zhou K, Shaw RM, Hong T. 2020. Exogenous cardiac bridging integrator 1 benefits mouse hearts with pre-existing pressure overload-induced heart failure. *Front. Physiol.* 11:708
95. Lyon AR, Nikolaev VO, Miragoli M, Sikkel MB, Paur H, et al. 2012. Plasticity of surface structures and β_2-adrenergic receptor localization in failing ventricular cardiomyocytes during recovery from heart failure. *Circ. Heart Fail.* 5:357–65
96. Ohtsuka T, Nakanishi H, Ikeda W, Satoh A, Momose Y, et al. 1998. Nexilin: a novel actin filament-binding protein localized at cell-matrix adherens junction. *J. Cell Biol.* 143:1227–38
97. Hassel D, Dahme T, Erdmann J, Meder B, Huge A, et al. 2009. Nexilin mutations destabilize cardiac Z-disks and lead to dilated cardiomyopathy. *Nat. Med.* 15:1281–88
98. Spinozzi S, Liu C, Chen Z, Feng W, Zhang L, et al. 2020. Nexilin is necessary for maintaining the transverse-axial tubular system in adult cardiomyocytes. *Circ. Heart Fail.* 13:e006935
99. Liu C, Spinozzi S, Feng W, Chen Z, Zhang L, et al. 2020. Homozygous G650del nexilin variant causes cardiomyopathy in mice. *JCI Insight* 5:e138780
100. Aherrahrou Z, Schlossarek S, Stoelting S, Klinger M, Geertz B, et al. 2016. Knock-out of nexilin in mice leads to dilated cardiomyopathy and endomyocardial fibroelastosis. *Basic Res. Cardiol.* 111:6
101. Wang H, Li Z, Wang J, Sun K, Cui Q, et al. 2010. Mutations in *NEXN*, a Z-disc gene, are associated with hypertrophic cardiomyopathy. *Am. J. Hum. Genet.* 87:687–93
102. Liu C, Spinozzi S, Chen JY, Fang X, Feng W, et al. 2019. Nexilin is a new component of junctional membrane complexes required for cardiac t-tubule formation. *Circulation* 140:55–66
103. Moore ED, Voigt T, Kobayashi YM, Isenberg G, Fay FS, et al. 2004. Organization of Ca^{2+} release units in excitable smooth muscle of the guinea-pig urinary bladder. *Biophys. J.* 87:1836–47
104. Somlyo AP. 1985. Excitation-contraction coupling and the ultrastructure of smooth muscle. *Circ. Res.* 57:497–507
105. Nelson MT, Cheng H, Rubart M, Santana LF, Bonev AD, et al. 1995. Relaxation of arterial smooth muscle by calcium sparks. *Science* 270:633–37
106. Wellman GC, Nelson MT. 2003. Signaling between SR and plasmalemma in smooth muscle: sparks and the activation of Ca^{2+}-sensitive ion channels. *Cell Calcium* 34:211–29
107. Herrera GM, Heppner TJ, Nelson MT. 2001. Voltage dependence of the coupling of Ca^{2+} sparks to BK_{Ca} channels in urinary bladder smooth muscle. *Am. J. Physiol. Cell Physiol.* 280:C481–90
108. Gonzales AL, Amberg GC, Earley S. 2010. Ca^{2+} release from the sarcoplasmic reticulum is required for sustained TRPM4 activity in cerebral artery smooth muscle cells. *Am. J. Physiol. Cell Physiol.* 299:C279–88
109. Earley S, Waldron BJ, Brayden JE. 2004. Critical role for transient receptor potential channel TRPM4 in myogenic constriction of cerebral arteries. *Circ. Res.* 95:922–29
110. Leblanc N, Forrest AS, Ayon RJ, Wiwchar M, Angermann JE, et al. 2015. Molecular and functional significance of Ca^{2+}-activated Cl^- channels in pulmonary arterial smooth muscle. *Pulm. Circ.* 5:244–68
111. Pritchard HAT, Gonzales AL, Pires PW, Drumm BT, Ko EA, et al. 2017. Microtubule structures underlying the sarcoplasmic reticulum support peripheral coupling sites to regulate smooth muscle contractility. *Sci. Signal.* 10:eaan2694

112. Pritchard HAT, Griffin CS, Yamasaki E, Thakore P, Lane C, et al. 2019. Nanoscale coupling of junctophilin-2 and ryanodine receptors regulates vascular smooth muscle cell contractility. *PNAS* 116:21874–81
113. Saeki T, Suzuki Y, Yamamura H, Takeshima H, Imaizumi Y. 2019. A junctophilin-caveolin interaction enables efficient coupling between ryanodine receptors and BK_{Ca} channels in the Ca^{2+} microdomain of vascular smooth muscle. *J. Biol. Chem.* 294:13093–105
114. Suzuki Y, Yamamura H, Ohya S, Imaizumi Y. 2013. Caveolin-1 facilitates the direct coupling between large conductance Ca^{2+}-activated K^+ (BK_{Ca}) and Cav1.2 Ca^{2+} channels and their clustering to regulate membrane excitability in vascular myocytes. *J. Biol. Chem.* 288:36750–61
115. Krishnan V, Ali S, Gonzales AL, Thakore P, Griffin CS, et al. 2022. STIM1-dependent peripheral coupling governs the contractility of vascular smooth muscle cells. *eLife* 11:e70278
116. Rosenbluth J. 1962. The fine structure of acoustic ganglia in the rat. *J. Cell Biol.* 12:329–59
117. Rosenbluth J. 1962. Subsurface cisterns and their relationship to the neuronal plasma membrane. *J. Cell Biol.* 13:405–21
118. Henkart M, Landis DM, Reese TS. 1976. Similarity of junctions between plasma membranes and endoplasmic reticulum in muscle and neurons. *J. Cell Biol.* 70:338–47
119. Wu Y, Whiteus C, Xu CS, Hayworth KJ, Weinberg RJ, et al. 2017. Contacts between the endoplasmic reticulum and other membranes in neurons. *PNAS* 114:E4859–67
120. BRAIN Init. Cell Census Netw. 2021. A multimodal cell census and atlas of the mammalian primary motor cortex. *Nature* 598:86–102
121. Berridge MJ. 1998. Neuronal calcium signaling. *Neuron* 21:13–26
122. Manita S, Ross WN. 2009. Synaptic activation and membrane potential changes modulate the frequency of spontaneous elementary Ca^{2+} release events in the dendrites of pyramidal neurons. *J. Neurosci.* 29:7833–45
123. Berrout J, Isokawa M. 2009. Homeostatic and stimulus-induced coupling of the L-type Ca^{2+} channel to the ryanodine receptor in the hippocampal neuron in slices. *Cell Calcium* 46:30–38
124. Miyazaki K, Ross WN. 2013. Ca^{2+} sparks and puffs are generated and interact in rat hippocampal CA1 pyramidal neuron dendrites. *J. Neurosci.* 33:17777–88
125. Vierra NC, Kirmiz M, van der List D, Santana LF, Trimmer JS. 2019. Kv2.1 mediates spatial and functional coupling of L-type calcium channels and ryanodine receptors in mammalian neurons. *eLife* 8:e49953
126. Jacobs JM, Meyer T. 1997. Control of action potential-induced Ca^{2+} signaling in the soma of hippocampal neurons by Ca^{2+} release from intracellular stores. *J. Neurosci.* 17:4129–35
127. Irie T, Trussell LO. 2017. Double-nanodomain coupling of calcium channels, ryanodine receptors, and BK channels controls the generation of burst firing. *Neuron* 96:856–70.e4
128. Mandikian D, Bocksteins E, Parajuli LK, Bishop HI, Cerda O, et al. 2014. Cell type-specific spatial and functional coupling between mammalian brain Kv2.1 K^+ channels and ryanodine receptors. *J. Comp. Neurol.* 522:3555–74
129. Antonucci DE, Lim ST, Vassanelli S, Trimmer JS. 2001. Dynamic localization and clustering of dendritic Kv2.1 voltage-dependent potassium channels in developing hippocampal neurons. *Neuroscience* 108:69–81
130. Misonou H, Mohapatra DP, Trimmer JS. 2005. Kv2.1: a voltage-gated K^+ channel critical to dynamic control of neuronal excitability. *Neurotoxicology* 26:743–52
131. Fakler B, Adelman JP. 2008. Control of K_{Ca} channels by calcium nano/microdomains. *Neuron* 59:873–81
132. Indriati DW, Kamasawa N, Matsui K, Meredith AL, Watanabe M, Shigemoto R. 2013. Quantitative localization of $Ca_V2.1$ (P/Q-type) voltage-dependent calcium channels in Purkinje cells: somatodendritic gradient and distinct somatic coclustering with calcium-activated potassium channels. *J. Neurosci.* 33:3668–78
133. Whitt JP, McNally BA, Meredith AL. 2018. Differential contribution of Ca^{2+} sources to day and night BK current activation in the circadian clock. *J. Gen. Physiol.* 150:259–75
134. Barbara JG. 2002. IP_3-dependent calcium-induced calcium release mediates bidirectional calcium waves in neurones: functional implications for synaptic plasticity. *Biochim. Biophys. Acta Proteins Proteom.* 1600:12–18

135. Yamasaki-Mann M, Demuro A, Parker I. 2013. Cytosolic [Ca^{2+}] regulation of InsP_3-evoked puffs. *Biochem. J.* 449:167–73
136. Thillaiappan NB, Chavda AP, Tovey SC, Prole DL, Taylor CW. 2017. Ca^{2+} signals initiate at immobile IP_3 receptors adjacent to ER-plasma membrane junctions. *Nat. Commun.* 8:1505
137. Ross CA, Meldolesi J, Milner TA, Satoh T, Supattapone S, Snyder SH. 1989. Inositol 1,4,5-trisphosphate receptor localized to endoplasmic reticulum in cerebellar Purkinje neurons. *Nature* 339:468–70
138. Takei K, Stukenbrok H, Metcalf A, Mignery GA, Sudhof TC, et al. 1992. Ca^{2+} stores in Purkinje neurons: endoplasmic reticulum subcompartments demonstrated by the heterogeneous distribution of the $InsP_3$ receptor, Ca^{2+}-ATPase, and calsequestrin. *J. Neurosci.* 12:489–505
139. Kaufmann WA, Ferraguti F, Fukazawa Y, Kasugai Y, Shigemoto R, et al. 2009. Large-conductance calcium-activated potassium channels in Purkinje cell plasma membranes are clustered at sites of hypolemmal microdomains. *J. Comp. Neurol.* 515:215–30
140. Benedeczky I, Molnar E, Somogyi P. 1994. The cisternal organelle as a Ca^{2+}-storing compartment associated with GABAergic synapses in the axon initial segment of hippocampal pyramidal neurones. *Exp. Brain Res.* 101:216–30
141. Lipkin AM, Cunniff MM, Spratt PWE, Lemke SM, Bender KJ. 2021. Functional microstructure of Ca_v-mediated calcium signaling in the axon initial segment. *J. Neurosci.* 41:3764–76
142. Spacek J, Harris KM. 1997. Three-dimensional organization of smooth endoplasmic reticulum in hippocampal CA1 dendrites and dendritic spines of the immature and mature rat. *J. Neurosci.* 17:190–203
143. Nishi M, Sakagami H, Komazaki S, Kondo H, Takeshima H. 2003. Coexpression of junctophilin type 3 and type 4 in brain. *Brain Res. Mol. Brain Res.* 118:102–10
144. Nishi M, Hashimoto K, Kuriyama K, Komazaki S, Kano M, et al. 2002. Motor discoordination in mutant mice lacking junctophilin type 3. *Biochem. Biophys. Res. Commun.* 292:318–24
145. Seixas AI, Holmes SE, Takeshima H, Pavlovich A, Sachs N, et al. 2012. Loss of junctophilin-3 contributes to Huntington disease-like 2 pathogenesis. *Ann. Neurol.* 71:245–57
146. Kakizawa S, Kishimoto Y, Hashimoto K, Miyazaki T, Furutani K, et al. 2007. Junctophilin-mediated channel crosstalk essential for cerebellar synaptic plasticity. *EMBO J.* 26:1924–33
147. Holmes SE, O'Hearn E, Rosenblatt A, Callahan C, Hwang HS, et al. 2001. A repeat expansion in the gene encoding junctophilin-3 is associated with Huntington disease-like 2. *Nat. Genet.* 29:377–78
148. Wilburn B, Rudnicki DD, Zhao J, Weitz TM, Cheng Y, et al. 2011. An antisense CAG repeat transcript at JPH3 locus mediates expanded polyglutamine protein toxicity in Huntington's disease-like 2 mice. *Neuron* 70:427–40
149. Lancaster B, Nicoll RA. 1987. Properties of two calcium-activated hyperpolarizations in rat hippocampal neurones. *J. Physiol.* 389:187–203
150. Adelman JP, Maylie J, Sah P. 2012. Small-conductance Ca^{2+}-activated K^+ channels: form and function. *Annu. Rev. Physiol.* 74:245–69
151. Akita T, Kuba K. 2000. Functional triads consisting of ryanodine receptors, Ca^{2+} channels, and Ca^{2+}-activated K^+ channels in bullfrog sympathetic neurons. Plastic modulation of action potential. *J. Gen. Physiol.* 116:697–720
152. Moriguchi S, Nishi M, Komazaki S, Sakagami H, Miyazaki T, et al. 2006. Functional uncoupling between Ca^{2+} release and afterhyperpolarization in mutant hippocampal neurons lacking junctophilins. *PNAS* 103:10811–16
153. Tedoldi A, Ludwig P, Fulgenzi G, Takeshima H, Pedarzani P, Stocker M. 2020. Calcium-induced calcium release and type 3 ryanodine receptors modulate the slow afterhyperpolarising current, sIAHP, and its potentiation in hippocampal pyramidal neurons. *PLOS ONE* 15:e0230465
154. Luo T, Li L, Peng Y, Xie R, Yan N, et al. 2021. The MORN domain of junctophilin2 regulates functional interactions with small-conductance Ca^{2+}-activated potassium channel subtype2 (SK2). *Biofactors* 47:69–79
155. Sahu G, Wazen RM, Colarusso P, Chen SRW, Zamponi GW, Turner RW. 2019. Junctophilin proteins tether a Cav1-RyR2-KCa3.1 tripartite complex to regulate neuronal excitability. *Cell Rep.* 28:2427–42.e6
156. Perni S, Beam K. 2021. Neuronal junctophilins recruit specific Cav and RyR isoforms to ER-PM junctions and functionally alter $Ca_V2.1$ and $Ca_V2.2$. *eLife* 10:e64249

157. Vacher H, Mohapatra DP, Trimmer JS. 2008. Localization and targeting of voltage-dependent ion channels in mammalian central neurons. *Physiol. Rev.* 88:1407–47
158. Liu PW, Bean BP. 2014. Kv2 channel regulation of action potential repolarization and firing patterns in superior cervical ganglion neurons and hippocampal CA1 pyramidal neurons. *J. Neurosci.* 34:4991–5002
159. Guan D, Armstrong WE, Foehring RC. 2013. Kv2 channels regulate firing rate in pyramidal neurons from rat sensorimotor cortex. *J. Physiol.* 591:4807–25
160. Malin SA, Nerbonne JM. 2002. Delayed rectifier K^+ currents, I_K, are encoded by Kv2 alpha-subunits and regulate tonic firing in mammalian sympathetic neurons. *J. Neurosci.* 22:10094–105
161. Trimmer JS. 1991. Immunological identification and characterization of a delayed rectifier K^+ channel polypeptide in rat brain. *PNAS* 88:10764–68
162. Trimmer JS. 2015. Subcellular localization of K^+ channels in mammalian brain neurons: remarkable precision in the midst of extraordinary complexity. *Neuron* 85:238–56
163. Bishop HI, Cobb MM, Kirmiz M, Parajuli LK, Mandikian D, et al. 2018. Kv2 ion channels determine the expression and localization of the associated AMIGO-1 cell adhesion molecule in adult brain neurons. *Front. Mol. Neurosci.* 11. **https://doi.org/10.3389/fnmol.2018.00001**
164. Du J, Tao-Cheng JH, Zerfas P, McBain CJ. 1998. The K^+ channel, Kv2.1, is apposed to astrocytic processes and is associated with inhibitory postsynaptic membranes in hippocampal and cortical principal neurons and inhibitory interneurons. *Neuroscience* 84:37–48
165. Bishop HI, Guan D, Bocksteins E, Parajuli LK, Murray KD, et al. 2015. Distinct cell- and layer-specific expression patterns and independent regulation of Kv2 channel subtypes in cortical pyramidal neurons. *J. Neurosci.* 35:14922–42
166. Fox PD, Haberkorn CJ, Akin EJ, Seel PJ, Krapf D, Tamkun MM. 2015. Induction of stable ER-plasma-membrane junctions by Kv2.1 potassium channels. *J. Cell Sci.* 128:2096–105
167. Johnson B, Leek AN, Sole L, Maverick EE, Levine TP, Tamkun MM. 2018. Kv2 potassium channels form endoplasmic reticulum/plasma membrane junctions via interaction with VAPA and VAPB. *PNAS* 115:E7331–40
168. Kirmiz M, Palacio S, Thapa P, King AN, Sack JT, Trimmer JS. 2018. Remodeling neuronal ER-PM junctions is a conserved nonconducting function of Kv2 plasma membrane ion channels. *Mol. Biol. Cell* 29:2410–32
169. Lim ST, Antonucci DE, Scannevin RH, Trimmer JS. 2000. A novel targeting signal for proximal clustering of the Kv2.1 K^+ channel in hippocampal neurons. *Neuron* 25:385–97
170. Rost BR, Schneider-Warme F, Schmitz D, Hegemann P. 2017. Optogenetic tools for subcellular applications in neuroscience. *Neuron* 96:572–603
171. Murphy SE, Levine TP. 2016. VAP, a versatile access point for the endoplasmic reticulum: review and analysis of FFAT-like motifs in the VAPome. *Biochim. Biophys. Acta Mol. Cell Biol. Lipids* 1861:952–61
172. Park KS, Mohapatra DP, Misonou H, Trimmer JS. 2006. Graded regulation of the Kv2.1 potassium channel by variable phosphorylation. *Science* 313:976–79
173. Misonou H, Mohapatra DP, Park EW, Leung V, Zhen D, et al. 2004. Regulation of ion channel localization and phosphorylation by neuronal activity. *Nat. Neurosci.* 7:711–18
174. Jegla T, Marlow HQ, Chen B, Simmons DK, Jacobo SM, Martindale MQ. 2012. Expanded functional diversity of Shaker K^+ channels in cnidarians is driven by gene expansion. *PLOS ONE* 7:e51366
175. O'Dwyer SC, Palacio S, Matsumoto C, Guarina L, Klug NR, et al. 2020. Kv2.1 channels play opposing roles in regulating membrane potential, Ca^{2+} channel function, and myogenic tone in arterial smooth muscle. *PNAS* 117:3858–66
176. Amberg GC, Santana LF. 2006. Kv2 channels oppose myogenic constriction of rat cerebral arteries. *Am. J. Physiol. Cell Physiol.* 291:C348–56
177. Vierra NC, O'Dwyer SC, Matsumoto C, Santana LF, Trimmer JS. 2021. Regulation of neuronal excitation-transcription coupling by Kv2.1-induced clustering of somatic L-type Ca^{2+} channels at ER-PM junctions. *PNAS* 118:e2110094118
178. Venditti R, Wilson C, De Matteis MA. 2021. Regulation and physiology of membrane contact sites. *Curr. Opin. Cell Biol.* 71:148–57
179. Li C, Qian T, He R, Wan C, Liu Y, Yu H. 2021. Endoplasmic reticulum-plasma membrane contact sites: regulators, mechanisms, and physiological functions. *Front. Cell Dev. Biol.* 9:627700

180. English AR, Voeltz GK. 2013. Endoplasmic reticulum structure and interconnections with other organelles. *Cold Spring Harb. Perspect. Biol.* 5:a013227
181. Rog-Zielinska EA, Scardigli M, Peyronnet R, Zgierski-Johnston CM, Greiner J, et al. 2021. Beat-by-beat cardiomyocyte T-tubule deformation drives tubular content exchange. *Circ. Res.* 128:203–15
182. Tao-Cheng JH. 2018. Activity-dependent decrease in contact areas between subsurface cisterns and plasma membrane of hippocampal neurons. *Mol. Brain* 11:23